BOREAS An international journal of Quaternary research

Cryptotephras in the Lateglacial ICDP Dead Sea sediment record and their implications for chronology

INA NEUGEBAUER, DANIELA MÜLLER, MARKUS J. SCHWAB, SIMON BLOCKLEY, CHRISTINE S. LANE, SABINE WULF, OONA APPELT AND ACHIM BRAUER

BOREAS

Neugebauer, I., Müller, D., Schwab, M. J., Blockley, S., Lane, C. S., Wulf, S., Appelt, O. & Brauer, A. 2021 (July): Cryptotephras in the Lateglacial ICDP Dead Sea sediment record and their implications for chronology. *Boreas*, Vol. 50, pp. 844–861. https://doi.org/10.1111/bor.12516. ISSN 0300-9483.

Due to a lack of visible tephras in the Dead Sea record, this unique palaeoenvironmental archive is largely unconnected to the well-established Mediterranean tephrostratigraphy. Here we present first results of the ongoing search for cryptotephras in the International Continental Drilling Program (ICDP) sediment core from the deep Dead Sea basin. This study focusses on the Lateglacial (~15–11.4 cal. ka BP), when Lake Lisan – the precursor of the Dead Sea – shrank from its glacial highstand to the Holocene low levels. We developed a glass shard separation protocol and counting procedure that is adapted to the extreme salinity and sediment recycling of the Dead Sea. Cryptotephra is abundant in the Dead Sea record (up to ~100 shards cm^{-3}), but often glasses are physically and/or chemically altered. Six glass samples from five tephra horizons reveal a heterogeneous geochemical composition, with mainly rhyolitic and some trachytic glasses potentially sourced from Italian, Aegean and Anatolian volcanoes. Most shards likely originate from the eastern Anatolian volcanic province and can be correlated using major element analyses with tephra deposits from swarm eruptions of the Süphan Volcano ~13 ka BP and with ashes from Nemrut Volcano, presumably the Lake Van V-16 volcanic layer at ~13.8 ka BP. In addition to glasses that match the TM-10-1 from Lago Grande di Monticchio (15 820±790 cal. a BP) tentatively correlated with the St. Angelo Tuff of Ischia, we further identified a cryptotephra with glass analyses which are chemically identical with those of the PhT1 tephra in the Philippon peat record (13.9–10.5 ka BP), and also a compositional match for the glass analyses of the Santorini Cape Riva Tephra (Y-2 marine tephra, 22 024±642 cal. a BP). These first results demonstrate the great potential of cryptotephrochronology in the Dead Sea record for improving its chronology and connecting the Levantine region to the Mediterranean tephra framework.

Ina Neugebauer (ina.neugebauer@gfz-potsdam.de) and Markus J. Schwab, Section Climate Dynamics and Landscape Evolution, GFZ German Research Centre for Geosciences, Telegrafenberg, Potsdam 14473, Germany; Daniela Müller and Achim Brauer, Section Climate Dynamics and Landscape Evolution, GFZ German Research Centre for Geosciences, Telegrafenberg, Potsdam 14473, Germany and Institute of Geosciences, University of Potsdam, Karl-Liebknecht-Str. 24–25, Potsdam 14476, Germany; Simon Blockley, Department of Geography, Royal Holloway University of London, Egham TW20 0EX, UK; Christine S. Lane, Department of Geography, University of Cambridge, Cambridge CB2 3EN, UK; Sabine Wulf, School of the Environment, Geography and Geosciences, University of Portsmouth, Portsmouth PO1 3HE, UK; Oona Appelt, Section Chemistry and Physics of Earth Materials, GFZ German Research Centre for Geosciences, Telegrafenberg, Potsdam 14473, Germany; *received 30th September 2020, accepted 22nd January 2021.*

In the drought-affected eastern Mediterranean region, a better understanding of the past hydroclimate variability is a prerequisite to improving our capability for estimating future changes of the water balance. In this respect, palaeoclimate records from marine or lake sediments provide invaluable information about natural hydroclimate changes. The hypersaline Dead Sea is a key palaeoclimate archive in the southeastern Mediterranean region, situated at a critical position between more humid Mediterranean climate and the hyper-arid Saharo-Arabian desert belt (e.g. Enzel *et al.* 2003; Migowski *et al.* 2006; Stein *et al.* 2011; Torfstein & Enzel 2017). As such, the Dead Sea is particularly sensitive for recording even small changes in the atmospheric circulation and precipitation by varying lake levels and sedimentary facies (e.g. Stein 2001). The ~450-m-long International Continental Drilling Program (ICDP) drill-core 5017-1, recovered from the deepest part of the Dead Sea, spans the last ~220 000 years (Stein *et al.* 2011; Neugebauer *et al.* 2014; Torfstein *et al.* 2015). Despite the recent refinement of the age model of the ICDP Dead Sea core (Goldstein *et al.* 2020), it still mainly relies on wiggle matching of $\delta^{18}O$ data and U–Th ages with comparably large dating uncertainties, hence, hampering the identification of lead- and lag-phase relationships of changing hydroclimate in comparison to other palaeoclimate records.

The timing and hydroclimatic response to abrupt climate change can only be unequivocally synchronized and compared between different climate records if each of their chronologies are precise and robust. In this respect, tephrochronology, i.e. identifying volcanic ash (tephra) of past volcanic eruptions in lacustrine and marine sediment records and using them as time-parallel markers, is the ideal method to achieve unambiguous synchronization (Lowe 2011; Davies *et al.* 2012; Lane *et al.* 2017). In recent years, methodological advances have enabled the identification of macroscopically invisible traces of volcanic ash – so-called cryptotephras – in sedimentary climate records, which have multiplied the

DOI 10.1111/bor.12516

number of identified tephras, in regions that can be several thousand kilometres away from the volcanic source (Lane *et al*. 2014; Davies 2015).

For the central and eastern Mediterranean region (Fig. 1A), comprehensive tephrostratigraphical efforts have led to a good understanding of the chemical compositions and spatial distribution of late Quaternary tephras deposited in marine and terrestrial sediment records (e.g. Keller *et al*. 1978; Narcisi & Vezzoli 1999; Bourne *et al*. 2010; Wulf *et al*. 2012; Matthews *et al*. 2015). The main volcanic source regions for late Quaternary tephra dispersals in the eastern Mediterranean region are the Italian volcanic provinces, the Hellenic Arc including Santorini, central Anatolia and eastern Anatolia (Fig. 1A). So far, there is no evidence for regionally significant volcanic eruptions and tephra dispersal from the Arabian volcanic province including the Harrat Ash Shaam field (Fig. 1A) of the southern Levant and northern Arabia in the late Quaternary (Hamann *et al*. 2010; Zanchetta *et al*. 2011). Therefore, the tephrostratigraphical work accomplished in recent decades is mainly based on the study of visible tephra layers identified in marine and lacustrine sediment records located in relative proximity to the highly active Italian and Aegean provinces (e.g. Keller *et al*. 1978; Federman & Carey 1980; Narcisi & Vezzoli 1999; Wulf *et al.* 2004, 2008, 2012, 2020; Bourne *et al*. 2010, 2015; Çağatay *et al*. 2015; Matthews *et al*. 2015; Tomlinson *et al*. 2015).

Despite being located in a favourable wind direction for receiving tephra from the central and eastern Mediterranean volcanoes via the westerlies, there are so far no tephra layers reported in palaeoclimate records from the southeastern Levantine region. The only exception is the Early Holocene (~9000 cal. a BP) Dikkartin eruption of the Erciyes Dagi in central Anatolia that was identified as a distal tephra layer in the Yammouneh palaeolake record in Lebanon, and in a marine sediment core from the SE Levantine Sea (Develle *et al*. 2009; Hamann *et al*. 2010). Recently, the first finding of this so-called 'S1' tephra as a cryptotephra in the Dead Sea and in the Tayma palaeolake record from NW Arabia allowed precise synchronization of these records and a discussion of lead- and lag-phase relationships of precipitation patterns in the Levantine-Arabian region during the Early Holocene humid period (Neugebauer *et al*. 2017). Moreover, this discovery encouraged a systematic search for tephra time-markers in the ICDP deep-basin core 5017-1 (Fig. 1B, C), with the aim of improving the chronology of the deep record and providing a tool for precise regional synchronization of proxy records.

The present study focusses on the last glacial–interglacial transition in the ICDP Dead Sea sediment core. Strong lake level fluctuations occurred at the last glacial precurser of the Dead Sea (Lake Lisan) during the Lateglacial; however, the hydroclimatic conditions in the central Levantine region in particular during Greenland Stadial 1 are uncertain (Stein *et al*. 2010). An improved chronology of the Dead Sea sediment record is a prerequisite for a precise synchronization with other palaeoclimate records, particularly in the eastern Mediterranean, in order to prove or disprove apparent large regional hydroclimatic differences like, for example a wet Younger Dryas in the Levant (Stein *et al*. 2010) and an arid Younger Dryas in Anatolia (e.g. Wick *et al*. 2003). This study aims at deciphering the Lateglacial hydroclimatic conditions in the Levantine region through the identification of cryptotephras in the Dead Sea sediment record and the improvement of its Lateglacial chronology. Such advanced insights into past regional climatic responses to global change are crucial to better anticipate possible future developments.

The ICDP Dead Sea record

Previous studies of the Dead Sea sediments were mainly restricted to sediment formations that are exposed at the margins of the lake (e.g. Bartov *et al*. 2002; Bookman (Ken-Tor) *et al.* 2004; Torfstein *et al*. 2009; Waldmann *et al*. 2009), or that were drilled along the western shoreline (Migowski *et al*. 2006). These outcrops and shallow cores, however, lack information especially about drier periods and low lake stands. Earlier attempts to drill in the deep basin were hampered by thick salt sequences that could not be penetrated (Heim *et al*. 1997). Therefore, a promising way to gain a continuous, long sediment record from the deep Dead Sea basin was through an ICDP drilling. From the ICDP Dead Sea Deep Drilling Project (DSDDP; 'The Dead Sea as a Global Paleoenvironmental, Tectonic, and Seismological Archive'), a ~450-m-long sediment record was recovered from the deepest part of the Dead Sea basin in 2010/11, comprising a continuous record of the last ~220 000 years of climate history in the southern Levantine region (Stein *et al*. 2011; Neugebauer *et al*. 2014).

The efforts to establish a robust chronology for the exposed sequences of the Dead Sea lacustrine formations have continued for more than two decades, applying radiocarbon, U–Th dating and floating $\delta^{18}O$ stratigraphy methods (see Stein & Goldstein 2006 for an overview; Torfstein *et al*. 2009, 2013a). Accordingly, this approach has also been applied to constrain the chronology of the ICDP deep core 5017-1. For the upper ~150 m of the core, the age-depth model is based on 38 ^{14}C dates of terrestrial plant remains that provide a relatively solid chronology for the last ~50 ka, i.e. back to the limit of the radiocarbon dating method (Neugebauer *et al*. 2014, 2015; Kitagawa *et al*. 2017). Unfortunately, this chronology includes unknown uncertainties because all dated plant remains could only be extracted from the base of turbidites so that reworking and resulting age/depth reversals cannot be excluded. Slumping of sediments and erosion by mass-transport deposits are very

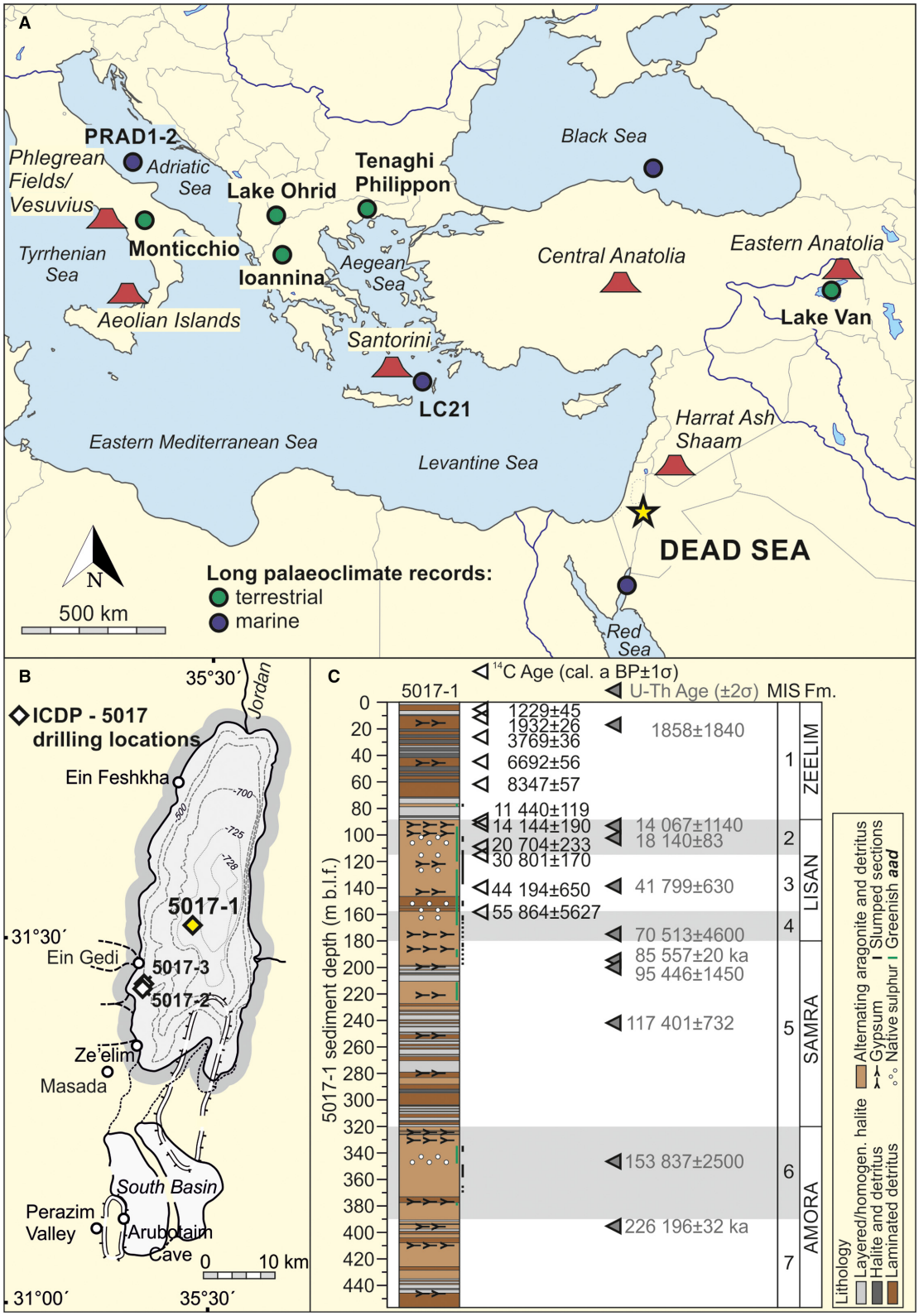

Fig. 1. A. Distribution map of central and eastern Mediterranean volcanic provinces and selected palaeoenvironmental sediment records with established late Quaternary tephrochronologies; the Dead Sea is highlighted (yellow star). B. Dead Sea map with drilling locations of the ICDP 5017 expedition (diamonds; core 5017-1 is analysed in this study) and selected onshore sites studied earlier (circles). C. Core 5017-1 lithostratigraphy (Neugebauer *et al.* 2014) and selected ^{14}C (Kitagawa *et al.* 2017) and U–Th ages (Torfstein *et al.* 2015); corresponding marine isotope stages (MIS) and Dead Sea sediment formations (Fm.) are also marked. [Colour figure can be viewed at www.boreas.dk]

common features in the core (Neugebauer *et al*. 2014; Kagan *et al*. 2018) and further add to the uncertainty of the chronology, but this can hardly be quantified. The age model of the older part of the core, reaching to ~220 000 years, was constructed by U–Th dating on primary aragonite that was combined with wiggle matching of stable oxygen isotope signals from aragonite layers and lithological changes that have been tied to exposed sediment formations, and to stable oxygen isotope data from the Soreq Cave speleothem and the LR04 global marine stack (Torfstein *et al*. 2015; Goldstein *et al*. 2020). Also, this approach is problematic, since (i) U–Th dating of authigenic carbonate requires a comprehensive correction procedure to account for the presence of detrital U and Th, and hydrogenic Th in Dead Sea sediments (Stein & Goldstein 2006 and references therein), which results in large age uncertainties of U–Th ages of up to several thousand years (Torfstein *et al*. 2013a); and because (ii) wiggle matching of oxygen isotope and lithological data to very different types of records is not independent.

Sediments of the ~450-m-long 5017-1 core, retrieved from a water depth of ~300 m (in 2010), mainly consist of alternating aragonite-detritus laminae, massive gypsum deposits, laminated marl, and halite sequences that are characteristic for the Amora (MIS 7-6), Samra (MIS 5), Lisan (MIS 4-2) and Zeelim (Holocene) sediment formations deposited in the Dead Sea basin (Fig. 1C; Neugebauer *et al*. 2014). One of the best-studied sections of the Dead Sea sediment formations is the Upper Lisan Formation, deposited in the Dead Sea basin during MIS 2 and building iconic sediment exposures in Masada (M1 outcrop) and the Perazim Valley (PZ1 outcrop) (e.g. Begin *et al*. 1980; Machlus *et al*. 2000; Bartov *et al*. 2002; Prasad *et al*. 2004, 2009; Torfstein *et al*. 2013b). The so-called 'White Cliff', finely laminated white aragonite and detritus sediments, formed during the Last Glacial Maximum when Lake Lisan was at its maximum highstand of ~160 m below sea level (b.s.l.; Torfstein *et al*. 2013b). The White Cliff is topped by the 'Upper and Additional Gypsum Units', which announce the Lake Lisan level retreat at the end of the last glacial at ~17.1–15.5±0.5 and at ~14.5±0.5 ka (Torfstein *et al*. 2013a) down to Holocene levels of ~400±30 m b.s.l. (Migowski *et al*. 2006). Due to this lake level decline, Lateglacial sediments and the transition to the Holocene between ~13 and 11 cal. ka BP are not exposed in the onshore deposits, but these can now be studied in the ICDP deep-basin core.

Material and methods

Sampling and glass shard extraction

Sediment cores of ICDP expedition 5017 are stored at the Marum Core Repository in Bremen, Germany. Sampling for glass shard analyses of cryptotephras of core 5017-1 is principally done in contiguous 5-cm steps with sample volumes of 5 cm^3, excluding mass-transported deposits (turbidites and slumps) thicker than 5 cm. Rock salts and other consolidated sediment sections that are too hard for sampling with a spatula were cut using a band saw at GFZ Potsdam, Germany.

The cryptotephra glass extraction protocol followed established physical and chemical separation procedures (Blockley *et al*. 2005), and has been further developed to account for the specific conditions of Dead Sea sediments. First, samples were repeatedly rinsed with deionized water in a shaking bath to dissolve salts and remove highly saline pore waters. Second, 10% HCl and 15% H_2O_2 solutions were added to remove carbonates and organic matter. This step was followed by wet-sieving into a 20–100 μm grain-size fraction, and sodium polytungstate (SPT) liquid density mineral separation, with volcanic glass shards being concentrated in the 2–2.55 g cm^{-3} fraction. Residual clays that disaggregated during this process were then removed by a second sieving through a 20-μm mesh.

The remaining sediment material still contains high concentrations of mineral grains (Fig. 2), which would prevent time-efficient glass shard counting of these samples. Therefore, *Lycopodium* spores (Fig. 2) with a defined number of spores per tablet (10 679±426 spores per tablet, batch no. 938934, Laboratory of Quaternary Geology University Lund, Sweden; Stockmarr 1971) were added to the samples. About 10% (at least 5%) of the total residue was mounted on glass slides for glass shard counting under a transmitted light polarization microscope. Along with counting *Lycopodium* spores in this subsample, the glass shard concentration per cubic centimetre of sediment or per gram dry weight can be estimated based on the given total number of spores (one tablet) in the total sample residue.

Geochemical characterization of tephra-derived glass

Glass shards of identified tephra horizons were picked under the microscope from the remaining ~90% of suspended sample material using a 100-μm-diameter gas-chromatography syringe attached to a micromanipulator (see Lane *et al*. 2014). Shards were transferred into single-hole-stubs, embedded in Araldite 2020 epoxy resin, ground and polished for electron probe microanalyses (EPMA). The major element composition of individual glass shards was measured using a JEOL JXA-8230 electron microprobe at GFZ Potsdam, Germany, with operating conditions of 15 kV voltage, 5 nA beam current, and a beam size of 5–10 μm depending on glass shard size. Exposure times were for each analysis 20 s for the elements Fe, Cl, Mn, Ti, Mg and P, and 10 s for Si, Al, K, Ca and Na. Instrumental calibration used natural mineral standards, and the glass standards Lipari obsidian (Hunt & Hill 1996; Kuehn *et al*. 2011) and MPI-Ding glasses ATHO-G, StHs-6-80-G and

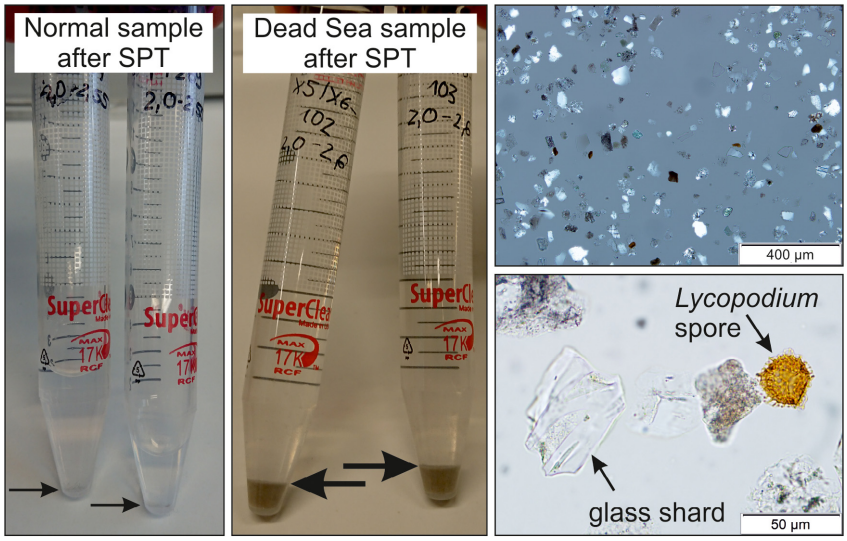

Fig. 2. Comparably large amounts of mineral grains (e.g. quartz, feldspars; upper right) in Dead Sea samples are left after physical-chemical treatment, requiring a specific protocol (adding *Lycopodium* spores to estimate tephra concentration from a ~10% aliquot of the 20–100 µm grain size and 2–2.55 g cm^{-3} density fraction). The comparison sample has been taken from evaporitic sediments of a high-altitude lake in Argentina. [Colour figure can be viewed at www.boreas.dk]

GOR-132-G (Jochum *et al*. 2006) were used during analytical runs to monitor the precision and accuracy of measurements (Table S1).

Lateglacial Dead Sea samples

For the present study, 56 samples between 89.30 and 94.09 m sediment depth below lake floor (m b.l.f.) from cores 5017-1-A-43 and 5017-1-A-44 were analysed for crypto-tephrostratigraphy, following the procedure illustrated above. These samples cover the top-most ~5 m of the Upper Lisan Formation in the ICDP core (Figs 1C, 3), i.e. immediately underlying the Early Holocene salt section (~73–89 m b.l.f. in 5017-1; Fig. 1C). From six of these samples, at least 10 glass shards per sample were measured by EPMA. Replicate measurements on a different set of glass shards from the sample were performed initially using 10 nA and later 5 nA beam currents for three samples, resulting in a total of 107 glass geochemical measurements (Table S1). Five values with raw totals of <90% were excluded from further evaluation.

Results

Glass shard counting

Of the 56 samples inspected here, 45 contain volcanic glass shards with concentrations of 4 to 107 shards cm^{-3} wet sediment (Fig. 3). Shards are concentrated in several 10–20 cm thick tephra horizons (TH) within finely laminated *aad* (alternating aragonite and detritus) sediments around 89.80, 90.05, 90.75, 92.00, 92.55, 93.30 and 93.95 m b.l.f. (Fig. 3). Even though turbidites thicker than 5 cm were excluded from cryptotephra sampling, evidence of smaller reworking events is still common and included in the samples. This reworking likely explains the physical alteration (rounding) of glass shards of at least 17 samples. In addition, particularly vesicular shards are often chemically altered at their surface and rims (Fig. 4), potentially as a result of the alkaline composition of the Dead Sea brine. The frequent occurrence of 'volcaniform' phytoliths, which have similar optical properties to these altered volcanic glasses, further complicates glass and hence tephra identification under the microscope. The maximum estimate of the shard concentration in Fig. 3 considers such ambiguous cases.

Glass shard morphologies

Glass shards are typically clear, devoid of microlites or other inclusions, and range in size mostly between 30 and 80 µm (Fig. 4). Some glass morphologies are preferentially found within specific TH. In the upper tephra horizons TH(89.80; 90.05; 90.75), glasses are mostly cuspate/butterfly-shaped or contain elongated vesicles (Fig. 4), and some are fluted. Tiny platy shards almost exclusively occur in TH(89.80). Glasses in TH(92.00) have cuspate or fluted shapes. In TH(92.55), glasses with elongated vesicles are noticeably thin. Vesicular and highly vesicular bubble-wall shards are characteristic in TH(93.30). Very thin butterfly shards occur in the lowermost tephra horizon TH(93.95).

Glass geochemical compositions

Major element EPMA data (n = 102; Table S1) of glass from the six samples analysed here show mostly rhyolitic and some trachytic glass compositions (Fig. 5). Seven

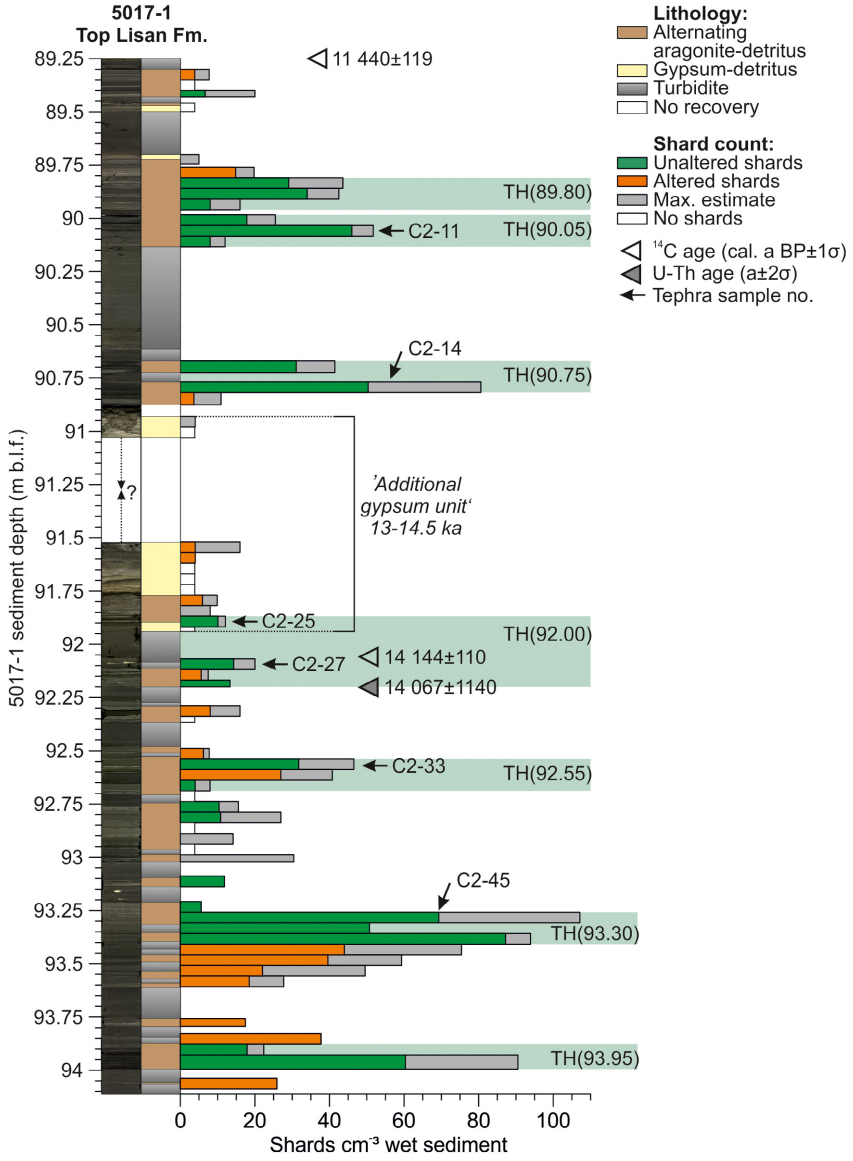

Fig. 3. Detailed lithology and glass counting results of the uppermost ~5 m of the Lisan Formation in the ICDP core 5017-1 from the deep Dead Sea basin. The alteration of shards has been defined by their optical appearance (rounded or sharp) under the microscope. Tephra horizons are highlighted by light green bars. Glass shards of the uppermost and lowermost tephra horizons could not be prepared for glass geochemical measurements because shards were too small (tiny platy shards in TH(89.80)), or had an unfavourable morphology (very thin butterfly shards in TH (93.95)). [Colour figure can be viewed at www.boreas.dk]

tephra populations can be distinguished that are mostly spread over several samples, i.e. they occur in several tephra horizons. These tephra populations (POP) are described in the following; their major element glass chemistry is shown in Figs 5 and 6 and summarized in Table 1. The analyses reported in the following text are on a normalized (volatile-free) basis (Table 1).

POP1 (trachytic). – Seven shards are trachytic in composition (five in sample 5017-C2-45, two in sample 5017-C2-25), close to the phonolite boundary, with 61.7–64.3 wt% SiO_2 and on average 6.5 wt% Na_2O and 6.5 wt% K_2O. These glasses are further characterized by ~18.7 wt% Al_2O_3, 0.5 wt% TiO_2 and 2.6 wt% FeO (total iron sum reported as FeO). CaO values in glass differ between the two samples, with ~1.1 wt% in sample 5017-1-C2-45 and ~1.8 wt% in sample 5017-C2-25 (Fig. 5).

POP2 (rhyolitic). – The composition of glass in population POP2 (n = 13) is characterized by a rhyolitic, close to dacitic, narrow cluster of 71.5–72.4 wt% SiO_2 and total alkalis of 6.6–8 wt%, whereas K_2O values are constant and low (~2.9 wt%). One glass shard with

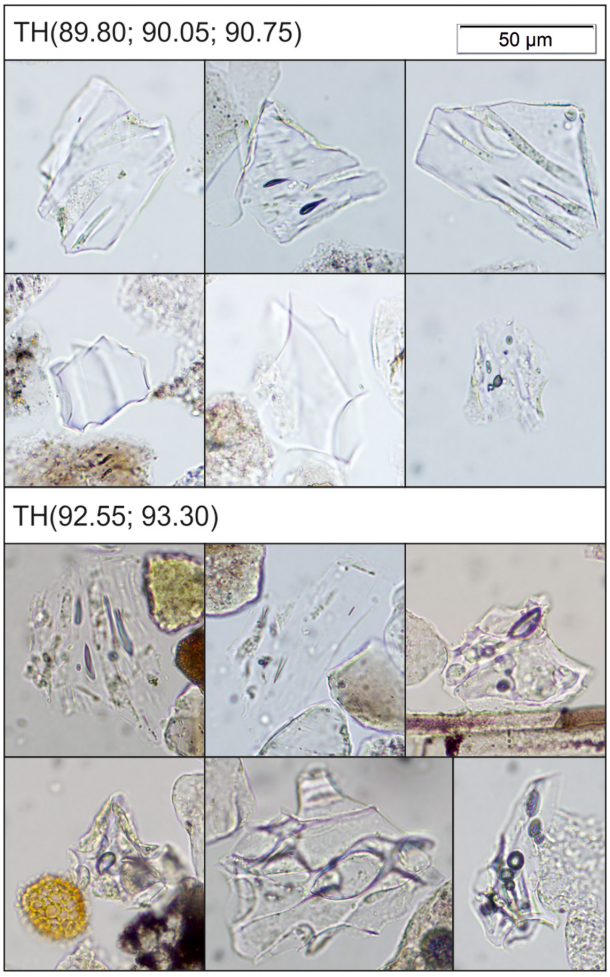

Fig. 4. Glass shard morphologies of different tephra horizons (TH); see text for details. [Colour figure can be viewed at www.boreas.dk]

lower SiO_2 (70 wt%), but high Na_2O (6.5 wt%) was assigned to this cluster as well (Fig. 6), as all other major elements occur in similar concentrations, e.g. ~14.7 wt% Al_2O_3, 3.1 wt% FeO, 0.5 wt% MgO and 1.7 wt% CaO (Table 1). Single glass shards of this population occur in nearly all analysed samples, except for sample 5017-C2-33, but most of them are located in sample 5017-C2-27 of TH(92.00) (Fig. 5).

POP3–POP7 (rhyolitic). – The majority of the glass shards analysed have rhyolitic compositions with 74–79 wt% SiO_2 and 6–9.5 wt% total alkalis (Fig. 5). Based on small differences in Ti, Al, Fe and Ca oxide contents and alkali ratios, five different tephra populations (POP3 to POP7) can be differentiated that describe n = 66 of all analysed shards (Fig. 6).

POP3 (n = 23) is characterized by particularly low TiO_2 (~0.05 wt%) and FeO (0.7 wt%), CaO is ~0.6 wt% and Na_2O is <4 wt%, and most glasses of this population were analysed in sample 5017-C2-33. Of the 14 analysed shards from this sample, 11 shards have compositions that fall into POP3 (Table S1).

POP4 (n = 16) shows very depleted CaO values (0.1–0.2 wt%), lower Al_2O_3 (~11.7 wt%) compared to POP3 (~12.9 wt%), higher FeO values (~2.6 wt%), and Na_2O >4 wt%. Glasses of POP4 occurred in all analysed samples; most in both the lowermost and uppermost samples 5017-C2-45 and 5017-C2-11, respectively.

The composition of POP5 (n = 13) is overall very similar to that of POP3 and POP4, with slightly higher TiO_2 (0.3 wt%) and Al_2O_3 (12.1 wt%), but similar FeO (2.4 wt%) compared to that of POP4, whereas CaO values of ~0.6 wt% compare with those of glass of POP3. However, the very low alkali-sum (~7 wt%) and higher K_2O/Na_2O (~1.6) ratio clearly distinguish POP5 from POP3 and POP4. Shards of this population occur in all analysed samples, except for sample 5017-C2-33.

POP6 (n = 8) shows the largest similarity with POP3; only SiO_2 is slightly lower (~75.6 wt%), and Al_2O_3 (13.4 wt%) and FeO (1.7 wt%) are somewhat higher. This population (POP6) mostly occurs in sample 5017-C2-27 of TH(92.00) and only occasionally in the overlying tephra horizons.

POP7 (n = 6) differs from POP3 to POP6 by having lower SiO_2 (72.7–76.8 wt%) and Al_2O_3 (8.2–11.7 wt%) concentrations, but much enhanced FeO values (4.6–5.9 wt%) (Fig. 6). Like POP6, most shards of this population were analysed in sample 5017-C2-27, while analyses of only single shards occur above.

Undefined glasses. – Sixteen glass compositions, eight of which were from sample 5017-C2-11, could not be assigned to any of the tephra populations defined above, and do not build a separate cluster (Figs 5, 6). Some of these glasses show apparent similarities with POP3, 4, 5 and 6, and others plot in between trachytic and rhyolitic compositions. One single glass shard is of trachydacitic composition.

Discussion

Lateglacial tephra record ~15–11 cal. ka BP in the Dead Sea

Considering that the Dead Sea in the southern Levantine region is largely influenced by westerly winds from the Mediterranean Sea, we would expect the majority of cryptotephras detected in the Dead Sea record to originate from Italian and Aegean volcanic centres. As the only visible tephra layer in the Levant – the Early Holocene 'S1' tephra from Erciyes volcano (Develle *et al.* 2009; Hamann *et al.* 2010), detected as a cryptotephra in the Dead Sea record (Neugebauer *et al.* 2017) – originates from central Anatolia, we also include the western, central and eastern Anatolian volcanic provinces as potential tephra sources.

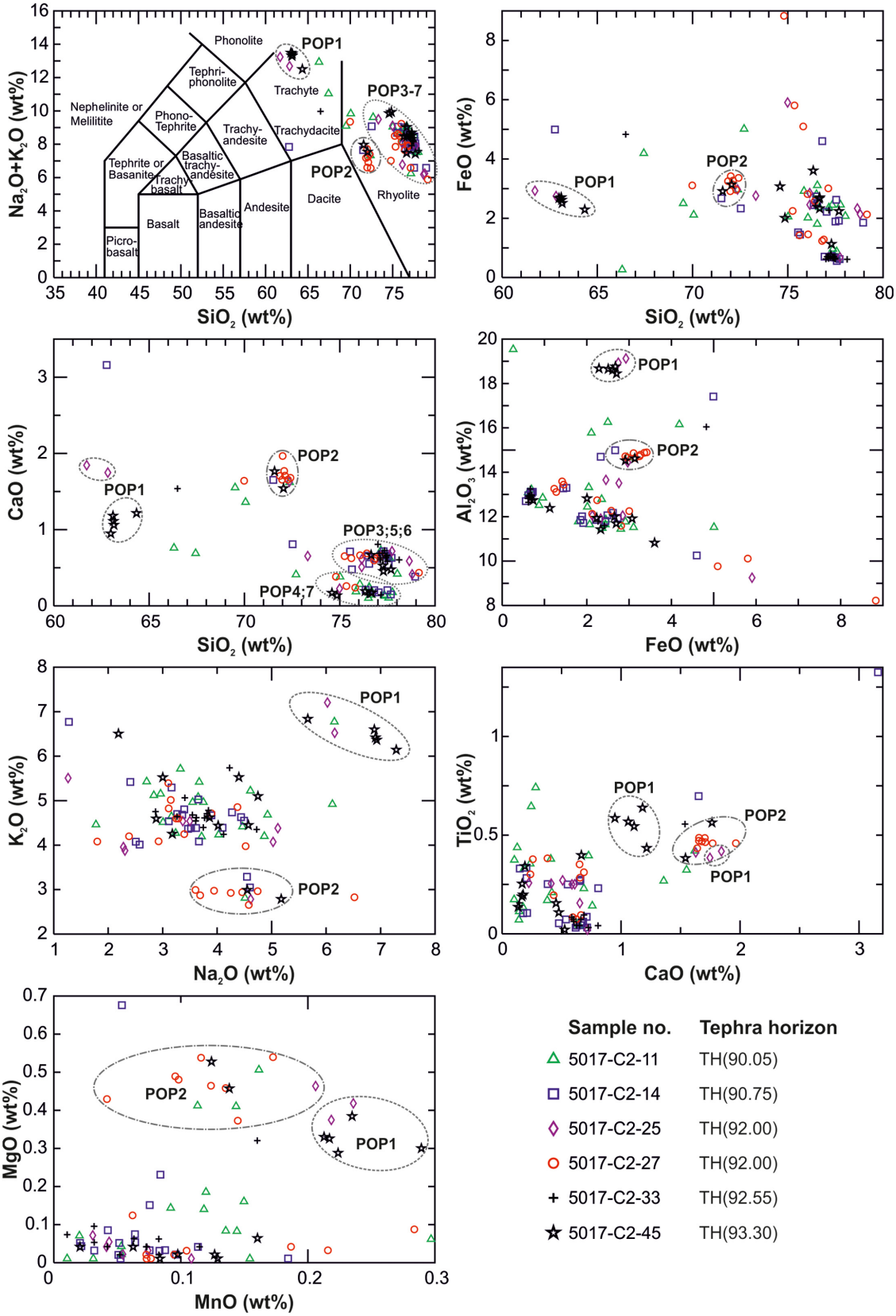

Fig. 5. Total alkali-silica diagram and bivariate elemental plots of EPMA normalized glass data from Lateglacial Dead Sea sediments (~15–11 cal. ka BP). Note that analytical errors are smaller than the symbol size. [Colour figure can be viewed at www.boreas.dk]

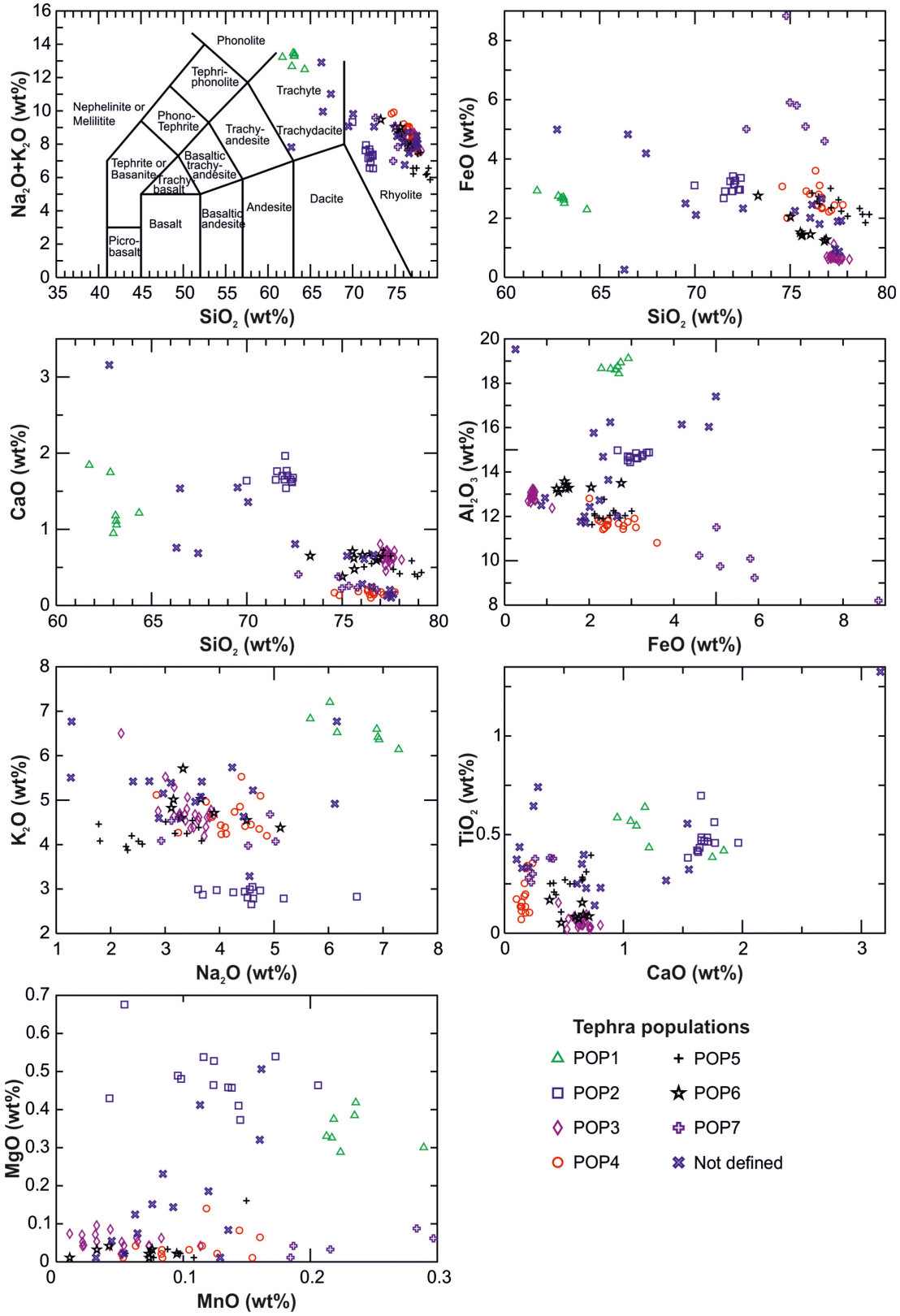

Fig. 6. Total alkali-silica diagram and bivariate elemental plots of EPMA normalized glass data of tephra populations identified in Lateglacial Dead Sea sediments (~15–11 cal. ka BP). Tephra populations were defined visually and by sorting the EPMA data table. Note that analytical errors are smaller than the symbol size. [Colour figure can be viewed at www.boreas.dk]

Table 1. Mean glass geochemical data in wt% (normalized, volatile-free) of the identified tephra populations (POP). Std = standard deviation; * = total iron is reported as FeO.

Tephra population	Total	SiO_2	TiO_2	Al_2O_3	FeO*	MnO	MgO	CaO	Na_2O	K_2O	P_2O_5	Na_2O+K_2O	K_2O/Na_2O
POP1 (n = 7)	93.76	63.04	0.51	18.74	2.64	0.23	0.35	1.30	6.55	6.58	0.05	13.13	1.02
std	1.11	0.71	0.09	0.21	0.19	0.02	0.04	0.32	0.55	0.32	0.02	0.36	0.13
POP2 (n = 13)	95.14	71.90	0.48	14.72	3.08	0.12	0.49	1.69	4.56	2.89	0.08	7.45	0.65
std	1.81	0.61	0.08	0.15	0.20	0.04	0.07	0.10	0.70	0.11	0.02	0.68	0.10
POP3 (n = 23)	95.75	77.39	0.05	12.93	0.68	0.04	0.05	0.64	3.43	4.77	0.02	8.20	1.43
std	1.6	0.26	0.03	0.20	0.10	0.03	0.02	0.07	0.38	0.46	0.02	0.30	0.37
POP4 (n = 16)	95.93	76.43	0.19	11.69	2.62	0.11	0.03	0.16	4.15	4.62	0.01	8.77	1.14
std	1.45	0.79	0.09	0.39	0.40	0.03	0.04	0.05	0.53	0.38	0.01	0.61	0.21
POP5 (n = 13)	92.96	77.59	0.26	12.08	2.41	0.10	0.02	0.55	2.77	4.21	0.01	6.97	1.60
std	1.54	1.01	0.06	0.26	0.32	0.03	0.04	0.12	0.64	0.21	0.01	0.74	0.39
POP6 (n = 8)	94.90	75.61	0.10	13.35	1.65	0.06	0.02	0.59	3.75	4.85	0.02	8.61	1.34
std	1.12	1.05	0.04	0.14	0.48	0.03	0.01	0.10	0.67	0.39	0.02	0.54	0.28
POP7 (n = 6)	93.92	75.08	0.33	9.85	5.87	0.24	0.04	0.29	3.96	4.32	0.01	8.28	1.15
std	2.26	1.25	0.05	1.00	1.40	0.04	0.03	0.08	0.88	0.29	0.02	0.88	0.28

Due to the large number and frequent activity of highly explosive volcanoes in the central and eastern Mediterranean during the Lateglacial and beyond, and because successive eruptions from the same source often have very similar glass compositions (e.g. Tomlinson *et al*. 2012a, 2015), assigning a particular volcanic eruption to a tephra population defined in our data is difficult. Also, a very distal cryptotephra record with low shard concentrations, as is the case for our record, may not represent the full compositional range of an eruption (Tomlinson *et al*. 2015), which might lead to false correlation, if the full geochemical range of a proximal deposit is also unknown. A further complication is the strong reworking of sediments in the Dead Sea basin, which requires extending the search for tephra correlatives beyond the Lateglacial period analysed here to consider those from older eruptions.

We first followed the attempt by Tomlinson *et al*. (2015) to discriminate the Mediterranean volcanic centres captured in our data, based on major element glass variations that are typical for different tectonic settings and volcanic provinces, before discussing the correlation of tephra populations with particular eruptives. In addition, we consulted the RESET Database (https://c14.arch.ox.ac.uk/resetdb/db.php; Bronk Ramsey *et al*. 2015b; Lowe *et al*. 2015) for available tephra data also from Anatolian provinces. Accordingly, we can distinguish at least three different sources – (i) the Neapolitan volcanic centre/and probably western Anatolia, (ii) Santorini, and (iii) eastern Anatolia/and probably central Anatolia (Fig. 7).

POP1 (Campanian and potentially western Anatolian volcanic provinces). – The trachytic composition of POP1 is similar to products of the Neapolitan volcanic district (Campi Flegrei, Ischia and Somma Vesuvius) that formed in a post-subduction setting (Tomlinson *et al*. 2015). Chemical biplots of Ca-Si, Na/K-Ca and Ca-Mg oxides, which are useful to discriminate Neapolitan volcanic products, place the five glass shards of POP1 from sample 5017-C2-45 that have low CaO (~1.1 wt%) in the field of the Ischia Island (Tomlinson *et al*. 2015). We found a good correlation of four glasses of this low-Ca subgroup of POP1 (Fig. 8) with the glass analyses of Ischia tephra layer TM-10-1 (15 820±790 cal. a BP) in the Lago Grande di Monticchio (LGdM) record (Wulf *et al*. 2008), which was suggested to relate to the St. Angelo Tuff from the Campotese volcano of Ischia (17 800±3200 K/Ar a; Poli *et al*. 1987). Glass of the marine C-3 tephra in deep-sea cores in the Tyrrhenian Sea has similar age and trachytic composition (Paterne *et al*. 1988), and was considered to represent the same explosive event (Wulf *et al*. 2008). Finding the product of a sub-Plinian eruption in the Dead Sea record, more than 2000 km away from the source, is noteworthy. In addition, the cryptotephra age of ~14.5 cal. ka BP in the Deep Sea core (sample 5017-1-C2-45, TH(93.30)) would be younger than TM-10-1 by at least ~500 years. Therefore, a correlation of the low-CaO glasses of POP1 with those of the TM-10-1 tephra from Ischia must be considered with caution.

Two POP1 glasses in sample 5017-C2-25 (~1.8 wt% CaO) overlap with Campi Flegrei Campanian Ignimbrite (CI)/pre-CI products in Tomlinson *et al*. (2015), and are similar to the glass composition of the Campanian Ignimbrite super-eruption (~39 ka, marine Y-5 tephra) itself (e.g. Tomlinson *et al*. 2012a; Giaccio *et al*. 2017) (TM-18 in LGdM, Fig. 8; Wulf *et al*. 2004). However, CI glasses in this stratigraphical position in the Dead Sea record are unlikely, and Tomlinson *et al*. (2012a) reported that Post-CI/Pre-NYT (Neapolitan Yellow Tuff) tephras can hardly be discriminated based on major element compositions alone (see TM tephra layers of LGdM originating from the Phlegrean fields in Fig. 8; Wulf *et al*. 2004, 2008). Therefore, we do not consider the CI as a likely source of the two 'high-CaO'

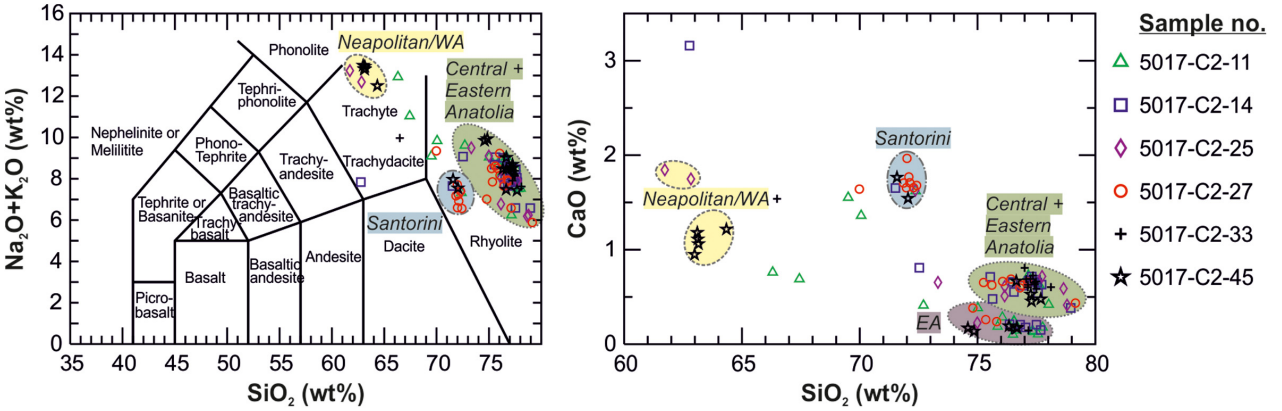

Fig. 7. Discrimination of Mediterranean volcanic centres captured in tephra data of Lateglacial Dead Sea sediments (~15–11 cal. ka BP). Note that the highlighted fields do not represent the full range of geochemical glass compositions of tephras from Neapolitan, Santorini and western, central and eastern Anatolian volcanic centres, and that available proximal tephra data from central and eastern Anatolia largely overlap. Only glasses from Nemrut volcano (eastern Anatolia) can be discriminated due to characteristically low CaO. [Colour figure can be viewed at www.boreas.dk]

glasses of POP1, even though reworking of older CI glasses cannot be entirely excluded.

A widely dispersed trachytic phreato-plinian deposit is the Neapolitan Yellow Tuff (NYT, marine C-2 tephra) that is the product of a high-magnitude, caldera-forming eruption of Campi Flegrei (Deino *et al.* 2004; Siani *et al.* 2004). Its $^{40}Ar/^{39}Ar$ isochron age of 14.9±0.4 ka (2σ) (Deino *et al.* 2004) and revised age of 14 194±172 cal. a BP (Bronk Ramsey *et al.* 2015a), considering ^{14}C dating and varve counting in Lago Grande di Monticchio (Wulf *et al.* 2004, 2008), would make the NYT a likely candidate for correlation with POP1. However, the NYT was rather dispersed to the north and has never been reported from eastern Mediterranean archives (Bronk Ramsey *et al.* 2015a). The slight mismatch of the major element compositions of the NYT (TM-8 in LGdM, Fig. 8; Wulf *et al.* 2004) and POP1 leave us to reject the NYT as a tephra correlative.

Trachytic tephra of the western Anatolian Gölcük volcano (Isparta, SW Turkey; Platevoet *et al.* 2008; Çoban *et al.* 2019), located much closer to the Dead Sea than the Campanian province and with most recent activity during the Lateglacial ((U–Th)/He zircon eruption ages 14.1±0.5 and 12.9±0.4 ka, 1σ; Schmitt *et al.*

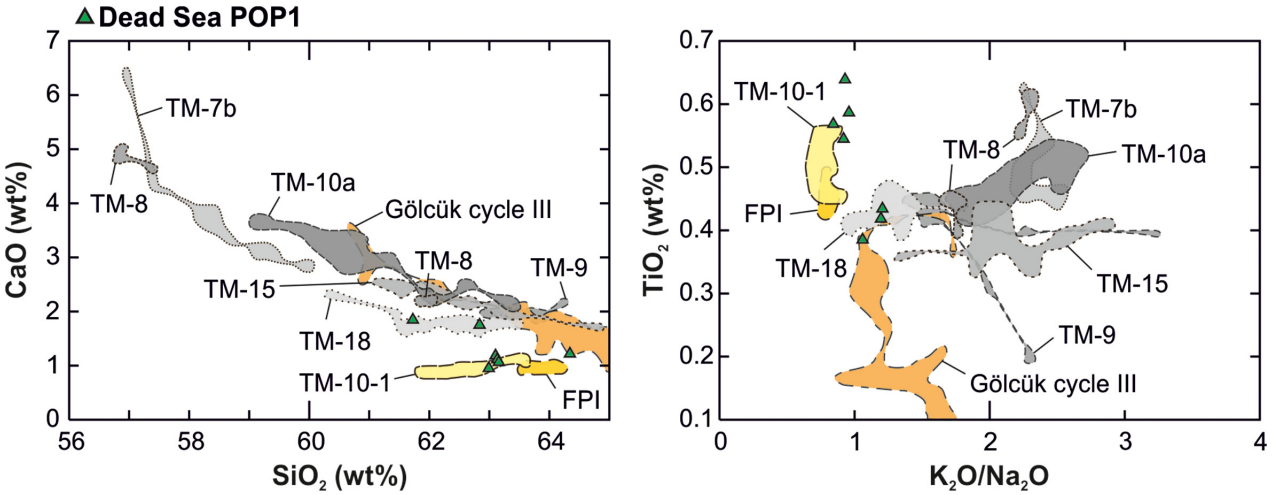

Fig. 8. Elemental biplots (normalized to 100%, volatile-free) of Dead Sea POP1 EPMA glass data (green triangles) compared with data of Ischia/Campanian eruptives, as recorded in the Lago Grande di Monticchio record (TM tephra layers; Wulf *et al.* 2004, 2008). Tephras related to the Phlegrean fields (grey shades): TM-7b = Pomici Principali; TM-8 = Neapolitan Yellow Tuff; TM-9 = Tufi Biancastri; TM-10a = Lagno Amendolare; TM-15 = marine Y-3 tephra; TM-18 = Campanian Ignimbrite (CI)/marine Y-5 tephra. Tephras related to Ischia (yellow shades): TM-10-1 = tentative correlation to St. Angelo Tuff/marine C-3 tephra (Wulf *et al.* 2008, and S. Wulf, unpublished data); FPI = Faro di Punta Imperatore in marine core PRAD 1-2, central Adriatic Sea (Bourne *et al.* 2010). Also shown are pumice data of Gölcük cycle III (orange field) from western Anatolia (Tomlinson *et al.* 2015). [Colour figure can be viewed at www.boreas.dk]

2014), is considered as a more likely candidate for correlation with 'high-CaO' glasses of POP1. Indeed, geochemical data of glass from the most recent eruption sequence Gölcük cycle III (Tomlinson *et al.* 2015) plot very close to our data, of which one glass lies directly within this field (Fig. 8).

POP2 (Santorini). – The major element composition of glass of the rhyolitic POP2 can be correlated with the active subduction setting of the Aegean volcanic province (Tomlinson *et al.* 2015), and more specifically with glass of the rhyodacitic Cape Riva Ash of Santorini (marine Y-2 tephra) (Federman & Carey 1980; Druitt *et al.* 1999; Fabbro *et al.* 2013; Wulf *et al.* 2020; Fig. 9). The Cape Riva eruption, radiocarbon-dated at 22 024±642 (2σ) cal. a BP (Bronk Ramsey *et al.* 2015a), formed prominent proximal pyroclastic fall deposits and far-spread distal tephra layers in the eastern Mediterranean region (e.g. St. Seymour *et al.* 2004; Satow *et al.* 2015; Wulf *et al.* 2020). Still, the appearance of the ~22 ka Cape Riva Ash in Lateglacial sediments of the Dead Sea is considered unlikely due to the large age difference that would imply considerable reworking of sediments.

However, there is distal evidence from the Tenaghi Philippon peat basin of northern Greece for deposition of a Lateglacial Santorini eruption that has glass chemically identical to that of Cape Riva tephra (St. Seymour *et al.* 2004; Wulf *et al.* 2018), but this has not yet been proven in the proximal or marine distal database (Druitt *et al.* 1999; Wulf *et al.* 2020). St. Seymour *et al.* (2004) described a visible tephra layer (PhT1) in the Philippi peat basin, radiocarbon-dated to 11 818±139 cal. a BP (IntCal13) but with conflicting estimates from ~13.9 to 10.5 cal. ka BP, which has glass with a chemical affinity to Y-2 and which was recognized some decimetres above the primary, several-centimetre-thick Y-2 (PhT2) tephra. Similarly, Wulf *et al.* (2018) identified two cryptotephra layers (that have comparably high shard concentrations >10 000 shards g^{-1} dwt; TP-05-7.07 and TP-05-7.26 in Fig. 9) that are chemically identical to those of the Cape Riva/Y-2 tephra in the Tenaghi Philippon TP-2005 core ~40–60 cm overlying the Y-2 tephra. Due to the lack of field and geochronological evidence for a Lateglacial eruption of Thera (Santorini) volcano, and because of the identical trace element composition of glass with that of the Y-2 tephra, the PhT1 tephra has been interpreted as a result of postdepositional recycling of Y-2 material (Wulf *et al.* 2018). Although we cannot exclude reworking in the Dead Sea sediments either, the occurrence of a cryptotephra with Cape Riva glass chemical affinity also in the Lateglacial sediments of the Dead Sea (sample 5017-C2-27 of TH(92.00); previously dated to ~14 cal. ka BP, see discussion below) might be another hint for a yet unknown Inter-Plinian eruption of the Santorini volcano during this period that so far has not yet been found in proximal sites.

POP3–POP6 (central/eastern Anatolia). – Glasses of the highly evolved, silicic tephra populations POP3 to POP6 overlap in their chemical composition with those of the products of several active subduction volcanic centres in the eastern Mediterranean; these are the

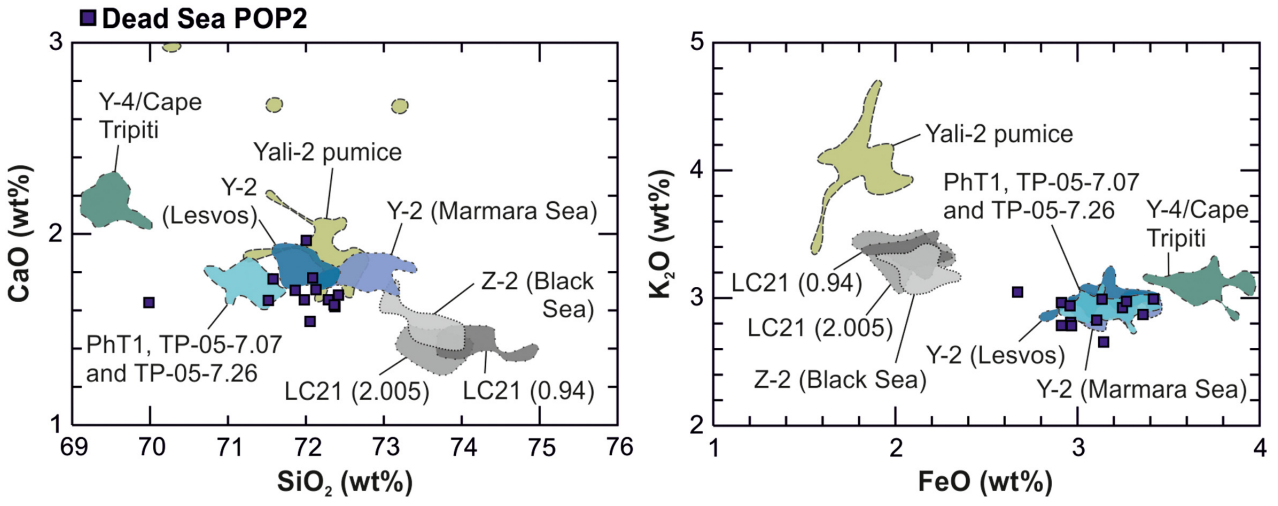

Fig. 9. Elemental biplots (normalized to 100%, volatile-free) of Dead Sea POP2 EPMA glass data (blue squares) compared with data of Santorini/Hellenic Arc eruptives. Minoan Ash/marine Z-2 tephra (Santorini; grey shades) recorded in SW Black Sea cores (Kwiecien *et al.* 2008) and in Aegean Sea core LC21 (LC21 (0.94)) (Satow *et al.* 2015); the older, Lateglacial cryptotephra layer LC (2.005) with identical chemical composition is also shown. Cape Riva/Y-2 tephra (Santorini; blue shades) recorded in the Marmara Sea (Wulf *et al.* 2002) and in Lesvos (Margari *et al.* 2007); the glass shards of cryptotephra layers of Lateglacial age in the Tenaghi Philippon record (PhT1, St. Seymour *et al.* 2004; TP-05-7.07 and TP-05-7.26, Wulf *et al.* 2018) have a similar, Cape Riva-like composition. The much older Hellenic Arc Yali-2 tephra (RESET Database, pumice collected inside Nisyros caldera by H. Kinvig) and the Cape Tripiti/Y-4 tephra from Santorini (Wulf *et al.* 2020) are plotted in green shades. [Colour figure can be viewed at www.boreas.dk]

Hellenic Arc islands Nisyros, Kos and Yali (without Santorini) and central Anatolia (Kuzucuoglu *et al*. 1998; Tomlinson *et al*. 2015), as well as eastern Anatolia (Sumita & Schmincke 2013b; Schmincke & Sumita 2014). Only for four major eruptives from Hellenic Arc volcanoes, geochemical glass data are available: the Yali-2 tephra, dated to ~35 ka BP based on orbitally tuned marine core KB28 (Vinci 1985), shows a similar glass chemical composition as that of the Cape Riva Ash (Tomlinson *et al*. 2015) and may be considered for potential correlation with POP2 (Fig. 9). The Nisyros Upper and Lower Pumices (~47 and 52 ka BP, respectively; Limburg & Varekamp 1991; Tomlinson *et al*. 2012b), and the Kos Plateau Tuff (KPT, marine W-3 tephra, ~166 ka BP; Bachmann *et al*. 2010) overlap in their glass shard compositions with POP3 to POP6. Even though we cannot entirely exclude these tephras as potential correlatives to our data, we also do not consider these as very likely due to their much older eruption ages.

The tephrostratigraphical framework for central and eastern Anatolian volcanic provinces is sparse in comparison to that of the comprehensive Italian and Aegean databases. While the Early Holocene Dikkartin, Perikartin and Karagüllü eruptives of Erciyes Dagi in central Anatolia (Hamann *et al*. 2010) do not match with POP3 to POP6 data (Fig. 10), eruptives of the central Anatolian Acigöl volcano at ~25–20 ka BP or younger, the so-called western Acigöl rhyolites, might fit in composition with our data (Schmitt *et al*. 2011; Siebel *et al*. 2011). However, only mean chemical analysis data of six rock samples are available for comparison (Fig. 10), restricting a proper interpretation of these data in comparison to our glass-based cryptotephra record. Kuzucuoglu *et al*. (1998) reported three rhyolitic tephras of Lateglacial age (GÖL T1, GÖL T5 and GÖL T11) from the Eski Acigöl lacustrine sequence and one (GÖCÜ 1 potentially correlating with the Korudagi Tuff of Acigöl) from the Göcü beach deposit sequence in the Konya Plain. The major element glass compositions, given only as mean values for these tephras (Kuzucuoglu *et al*. 1998), do not agree well with Dead Sea POPs when several elements are considered (Fig. 10).

Our POP3 to POP6 major element glass data show the best correlation with eastern Anatolian Süphan swarm eruptives around 13 cal. ka BP and with glass analyses of Nemrut Dagi ashes, as reported from tephra layers in the ICDP Lake Van sediment core (Schmincke & Sumita 2014). The Lateglacial Süphan tephra swarm occurred during a short time interval of ~338 years between ~13 078 and 12 740 varve years BP, labelled as V-8 to V-15 volcanic layers in Lake Van varved (annually laminated) sediments (Schmincke & Sumita 2014). POP3 and likely POP5 correlate with these chemically very similar Süphan eruptives around 13 cal. ka BP, and POP6 might correlate with V-13 that has glass with a somewhat higher FeO than other Süphan eruptives of this swarm (Fig. 10; Schmincke & Sumita 2014). POP4 most likely represents the V-16 layer of a Nemrut eruption ~13.8 cal. ka BP, as can be seen in the characteristically low CaO values (~0.2–0.3 wt%) of glass of the rhyolitic Nemrut tephras. However, higher FeO in glass of POP4 could also suggest a correlation to Nemrut V-17 that is dated to >30 ka BP in the Lake Van core. Schmincke & Sumita (2014) postulate a tephra gap between 30 ka BP (V-17) and ~14 ka BP (V-16); hence, a match with V-17 in our data would imply reworking of tephra over more than 15 000 years in the Dead Sea record, which we consider as highly unlikely. It should also be noted that only single representative values of glass compositions for Lake Van tephra layers are reported, which cannot illustrate the whole range of glass compositions of these tephras.

POP7 and 'not defined' glasses (not identified). – The tephra population POP7 and glasses that could not be defined here potentially originate from eruptives of central and eastern Anatolian volcanic centres as well (Fig. 10). Unfortunately, the current, very limited proximal glass chemical database does not allow any conclusive correlation with our cryptotephra-derived glass data set.

Implications for the Lateglacial chronology of the Dead Sea record

The Lateglacial is of particular interest for palaeoclimate research at the Dead Sea because several strong lake level drops occurred between the Last Glacial Maximum highstand of Lake Lisan and the Holocene low-level of the Dead Sea. However, the last glacial–interglacial transition (LGIT) could not be studied for its entire duration before the ICDP deep drilling because of the lack of exposed sediments dating to this time. This gap particularly concerns the sedimentological and hydroclimatic signature of the Greenland Stadial 1 (GS-1) in the Levantine region, which is under debate (Stein *et al*. 2010).

The oldest Holocene Dead Sea sediments comprise the 'Early Holocene salt section' that has been radiocarbon-dated in marginal shallow cores to between 10 and 11 cal. ka BP (Stein *et al*. 2010). In the ICDP core, this Early Holocene salt is evident at ~71 to 88.5 m sediment depth (Figs 1C, 11). No radiocarbon or U–Th ages exist from this section of the core, but a ~75-cm-thick turbidite directly below is radiocarbon-dated at its base at 89.25 m b.l.f. to 11 440±119 cal. a BP (Neugebauer *et al*. 2014; Kitagawa *et al*. 2017), supporting an age for the start of the salt sequence of ~11 cal. ka BP in the marginal cores (Stein *et al*. 2010) if significant reworking of the dated sample is excluded. So far, the only available age estimates for the LGIT in the ICDP core are from below a massive gypsum deposit at ~91–92 m b.l.f. (Fig. 11): a ^{14}C age of 14 144±110 cal. a BP retrieved from the base of a ~15-cm-thick turbidite at 92.06 m b.l.f. (Neugebauer

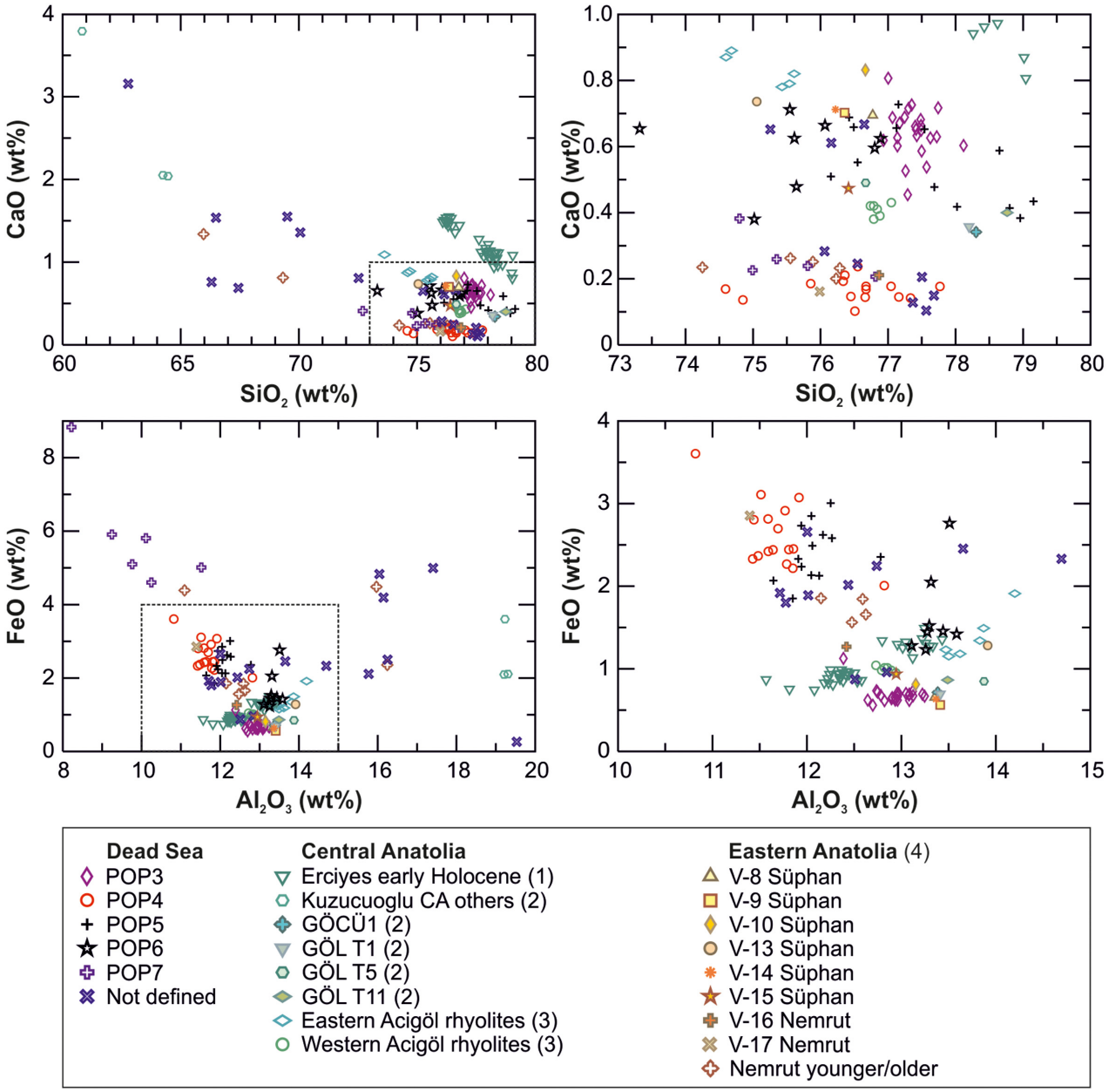

Fig. 10. Elemental biplots (normalized to 100%, volatile-free) of Dead Sea POP3–POP7 EPMA glass data (including 'not defined' glasses, i.e. glasses that do not correlate with glass of any tephra population) compared to data from central and eastern Anatolian volcanic provinces. Central Anatolia: (1) Early Holocene eruptions of Erciyes Dagi (Hamann *et al.* 2010); (2) GÖCÜ 1 (Korudagi tuff of Acigöl), GÖL T1, GÖL T5 and GÖL T11 (Acigöl) (Kuzucuoglu *et al.* 1998); (3) eastern Acigöl (~150–200 ka BP) and western Acigöl (~25–20 ka BP) rhyolites (Siebel *et al.* 2011). Eastern Anatolia: (4) Lateglacial Süphan swarm (V-8 to V-15 in Lake Van) and Nemrut data V-16 (~13.8 ka BP), V-17 (~30 ka BP), as well as younger (V3a–V6; Holocene) and older (V-18) Nemrut tephra layers in Lake Van (Schmincke & Sumita 2014). [Colour figure can be viewed at www.boreas.dk]

et al. 2014; Kitagawa *et al.* 2017) and an U–Th isochron age of 14 067±1140 a BP measured on aragonite at 92.20 m b.l.f. (Torfstein *et al.* 2015). These ages suggest deposition of this gypsum unit, labelled as 'Additional Gypsum Unit' (AGU) in the Masada section by Torfstein *et al.* (2013a), during Greenland Interstadial 1a-c. In contrast, our tephrochronological correlation provides evidence for a ~1000-years younger bottom-age of the gypsum deposit. Volcanic glass shards directly below the gypsum deposit (tephra horizons TH(92.00) and TH(92.55)) correlate with products of the Süphan swarm eruptions, which have been varve-dated at between 12 740 and 13 078 varve years BP in the Lake Van core (V8–V15 tephra layers) (Schmincke & Sumita 2014). Furthermore, we are confident that glass shards found at ~93 m b.l.f. in the ICDP core (TH(93.30))

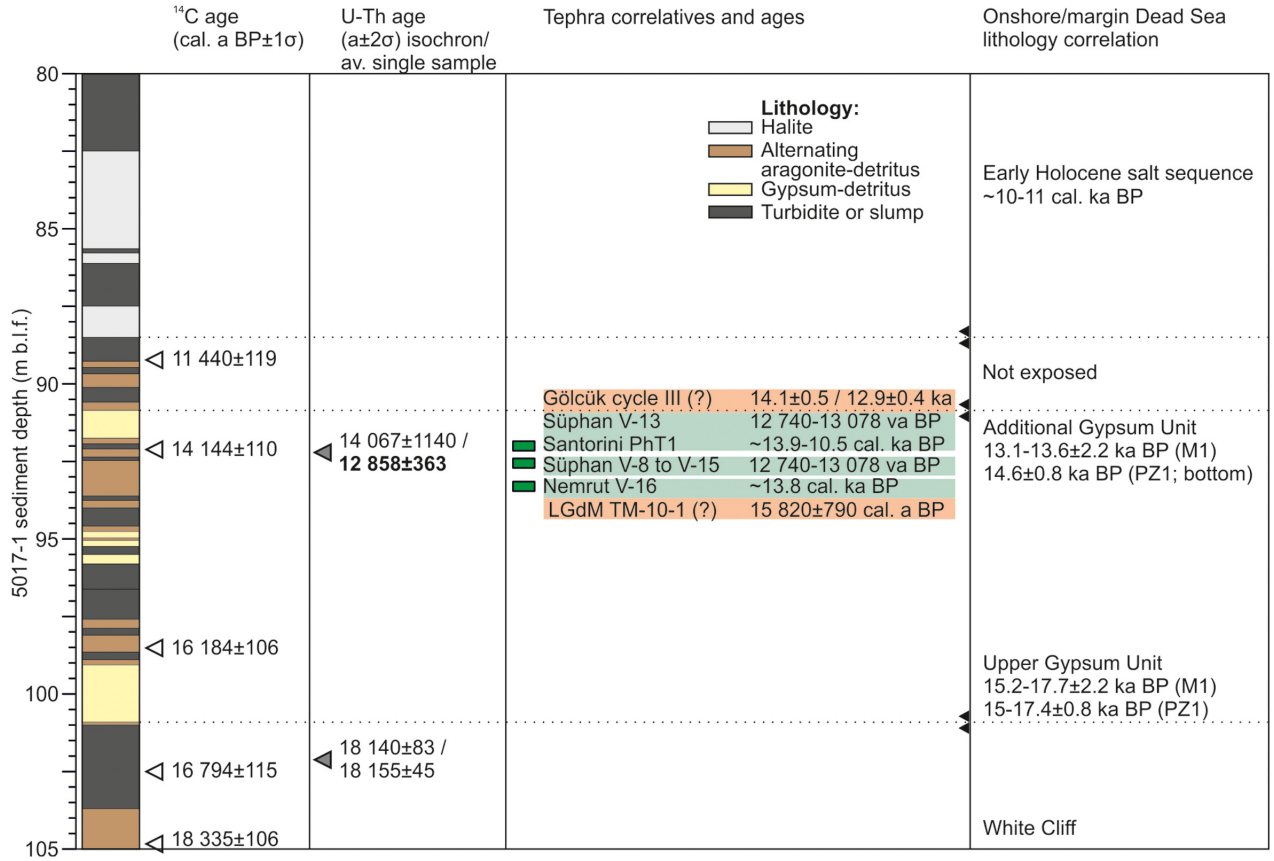

Fig. 11. Lithology, available ^{14}C and U–Th ages (Torfstein *et al.* 2015; Kitagawa *et al.* 2017), identified cryptotephras in the Lateglacial 5017-1 core (St. Seymour *et al.* 2004; Schmincke & Sumita 2014), and correlation of 5017-1 lithologies with onshore sediment formations. We also included tentative tephra correlations in this plot; these are TM-10-1 in the LGdM record (Wulf *et al.* 2008) that is located at the same sediment depth as Nemrut V-16, and Gölcük cycle III tephra at the same sediment depth as Süphan V-13 and Santorini PhT1. The Early Holocene salt sequence is the bottom-section of the Zeelim Formation, radiocarbon-dated to between 10 and 11 cal. ka BP in numerous shallow drill-cores at the western margin of the Dead Sea (Stein *et al.* 2010). The 'Additional' and 'Upper Gypsum Units' form the top of the last glacial Lisan Formation and have been dated by U–Th in outcrops at Masada (M1 section; Torfstein *et al.* 2013a) and Perazim Valley (PZ1 section; Haase-Schramm *et al.* 2004). va = varve years. [Colour figure can be viewed at www.boreas.dk]

correlate with those of the V-16 tephra layer in Lake Van, originating from an eruption of Nemrut Volcano at ~13.8 cal. ka BP (Schmincke & Sumita 2014). Our revised age for the gypsum deposit in the core further agrees within dating uncertainties with U–Th ages of ~13–14.5 ka BP for the corresponding onshore 'Additional Gypsum Unit' that has been dated at the M1 section in Masada and the PZ1 section in Perazim Valley (Figs 1B, 11; Haase-Schramm *et al.* 2004; Torfstein *et al.* 2013a). Moreover, the age supports the average single sample U–Th age of 12 858±363 a BP obtained at 92.20 m b.l.f. in the ICDP core (Torfstein *et al.* 2015) instead of the above-mentioned, parallel U–Th isochron age of 14 067±1140 a BP. Therefore, we are confident that the massive gypsum unit, which correlates with the AGU section at Masada, formed during the early GS-1 rather than during the Lateglacial interstadial (GI-1a-c) as previously suggested. Since the AGU represents the final deposits of the Lake Lisan highstand period, this further implies that the major lake level decline did not occur at the onset of the Lateglacial interstadial as previously assumed (Torfstein *et al.* 2013a) but only at around the transition to the Younger Dryas. Consequently, also previous interpretation of the Younger Dryas as a wet period in the Levant (Stein *et al.* 2010) must be questioned. An arid Younger Dryas as indicated by gypsum deposition is in accord with the observed coupling between millennial-scale lake level declines of the Dead Sea and cold Heinrich events in the North Atlantic (Torfstein *et al.* 2013b). This would reconcile the apparent contradiction of the Younger Dryas as the only cold period in the North Atlantic causing lake level rise (Stein *et al.* 2010) rather than decline of the Dead Sea. Furthermore, an arid Younger Dryas in the Levant is congruent with a dry eastern Mediterranean (Rossignol-Strick 1995) and major lake level lowering in Lake Van (Landmann *et al.* 1996; Wick *et al.* 2003) during that time.

Conclusions

In the Lateglacial (~11–15 cal. ka BP) time interval of the ICDP Dead Sea core, we have identified numerous cryptotephra horizons, from at least three different sources of Italian, Aegean and Anatolian volcanic centres. First glass geochemical data suggest that the majority of volcanic ash in the Dead Sea sediments originates from eruptions of the Anatolian volcanic provinces. Even though proximal Anatolian tephra data (glass shard analyses) for comparison are still limited, the identification of cryptotephra in the long Dead Sea record provides novel opportunities to advance the tephrostratigraphical framework in this region, e.g. not only through synchronizing the Dead Sea and Lake Van (eastern Anatolia) sediment records, but also with archaeological and palaeoenvironmental sites that are currently investigated in the Levant and in Arabia. Furthermore, the glass composition-based correlation of tephra populations in the Dead Sea with well-dated Lateglacial tephras of the Süphan and Nemrut volcanoes at Lake Van enabled us to improve the chronology of the Dead Sea record significantly, in a critical time-window for better understanding the hydroclimatic conditions in the region during abrupt climate changes at the end of the last glacial. The results of this study pave the way for extending the tephra work at the Dead Sea, and for synchronization with other important palaeoclimate records in the Mediterranean region, like Lago Grande di Monticchio, Italy, Lake Ohrid, Albania/Macedonia, Tenaghi Philippon, Greece, and Lake Van, Turkey.

Acknowledgements. – We like to thank Jan A. Piotrowski for editing this article, and David J. Lowe and an anonymous reviewer for their very constructive suggestions that helped to improve the quality. This study has received funding by the German Academic Exchange Service (DAAD postdoc grant to IN) and the German Research Foundation (DFG research grant to IN, grant no. NE 2295/1-1) and is a contribution to the projects 'TEPH-ME: CryptoTEPHrochronology in the ICDP Dead Sea deep core as a key to synchronise past hydroclimate changes in the eastern MEditerranean' and 'PALEX: Paleohydrology and Extreme Floods from the Dead Sea ICDP core' (DFG grant no. BR2208/13-1/-2). We thank our student helpers Miriam Seidel, Anna Beer (University Münster) and Daniel Redant (Free University Berlin) for assistance in the Potsdam Tephra Lab, and Brian Brademann and Nicolai Klitscher (both GFZ) for help with technical and practical issues. Part of the laboratory work was carried out in the Cambridge Tephra Lab during a research visit of IN in the Department of Geography, University of Cambridge, and we thank Alma Piermattei, Amy McGuire and Erin Martin-Jones for their help with method development. We confirm that there is no conflict of interest to declare for this study.

Author contributions. – IN, DM and MJS developed the project idea, and performed the sampling and sample preparation. IN and OA analysed glass shards using EPMA. Data evaluation was done by IN, DM, SB, CSL and SW. IN and AB wrote the manuscript with contributions from all co-authors.

Data availability statement. – Data of this article will be publicly available on PANGAEA.

References

Bachmann, O., Schoene, B., Schnyder, C. & Spikings, R. 2010: The $^{40}Ar/^{39}Ar$ and U/Pb dating of young rhyolites in the Kos-Nisyros volcanic complex, Eastern Aegean Arc, Greece: age discordance due to excess ^{40}Ar in biotite. *Geochemistry, Geophysics, Geosystems 11*. Q0AA08, https://doi.org/10.1029/2010GC003073.

Bartov, Y., Stein, M., Enzel, Y., Agnon, A. & Reches, Z. 2002: Lake levels and sequence stratigraphy of Lake Lisan, the Late Pleistocene precursor of the Dead Sea. *Quaternary Research 57*, 9–21.

Begin, Z., Nathan, Y. & Ehrlich, A. 1980: Stratigraphy and facies distribution in the Lisan Formation—new evidence from the area south of the Dead Sea, Israel. *Israel Journal of Earth Sciences 29*, 182–189.

Blockley, S. P. E., Pyne-O'Donnell, S. D. F., Lowe, J. J., Matthews, I. P., Stone, A., Pollard, A. M., Turney, C. S. M. & Molyneux, E. G. 2005: A new and less destructive laboratory procedure for the physical separation of distal glass tephra shards from sediments. *Quaternary Science Reviews 24*, 1952–1960.

Bookman (Ken-Tor), R., Enzel, Y., Agnon, A. & Stein, M. 2004: Late Holocene lake levels of the Dead Sea. *Geological Society of America Bulletin 116*, 555–571.

Bourne, A. J., Albert, P. G., Matthews, I. P., Trincardi, F., Wulf, S., Asioli, A., Blockley, S. P. E., Keller, J. & Lowe, J. J. 2015: Tephrochronology of core PRAD 1–2 from the Adriatic Sea: insights into Italian explosive volcanism for the period 200–80 ka. *Quaternary Science Reviews 116*, 28–43.

Bourne, A. J., Lowe, J. J., Trincardi, F., Asioli, A., Blockley, S. P. E., Wulf, S., Matthews, I. P., Piva, A. & Vigliotti, L. 2010: Distal tephra record for the last ca 105,000 years from core PRAD 1–2 in the central Adriatic Sea: implications for marine tephrostratigraphy. *Quaternary Science Reviews 29*, 3079–3094.

Bronk Ramsey, C., Albert, P. G., Blockley, S. P. E., Hardiman, M., Housley, R. A., Lane, C. S., Lee, S., Matthews, I. P., Smith, V. C. & Lowe, J. J. 2015a: Improved age estimates for key Late Quaternary European tephra horizons in the RESET lattice. *Quaternary Science Reviews 118*, 18–32.

Bronk Ramsey, C., Housley, R. A., Lane, C. S., Smith, V. C. & Pollard, A. M. 2015b: The RESET tephra database and associated analytical tools. *Quaternary Science Reviews 118*, 33–47.

Çağatay, M. N., Wulf, S., Sancar, Ü., Özmaral, A., Vidal, L., Henry, P., Appelt, O. & Gasperini, L. 2015: The tephra record from the Sea of Marmara for the last ca. 70 ka and its palaeoceanographic implications. *Marine Geology 361*, 96–110.

Çoban, H., Topuz, G., Roden, M. F., Hoang, N. & Schwarz, W. H. 2019: ^{40}Ar-^{39}Ar dating and petrology of monzonite ejecta in tephra from Quaternary Gölcük volcano (Isparta, SW Turkey): tear-related contrasting metasomatic symptoms in extensional mantle-derived magmas. *Lithos 330–331*, 160–176.

Davies, S. M. 2015: Cryptotephras: the revolution in correlation and precision dating. *Journal of Quaternary Science 30*, 114–130.

Davies, S. M., Abbott, P. M., Pearce, N. J. G., Wastegård, S. & Blockley, S. P. E. 2012: Integrating the INTIMATE records using tephrochronology: rising to the challenge. *Quaternary Science Reviews 36*, 11–27.

Deino, A. L., Orsi, G., de Vita, S. & Piochi, M. 2004: The age of the Neapolitan Yellow Tuff caldera-forming eruption (Campi Flegrei caldera – Italy) assessed by $^{40}Ar/^{39}Ar$ dating method. *Journal of Volcanology and Geothermal Research 133*, 157–170.

Develle, A.-L., Williamson, D., Gasse, F. & Walter-Simonnet, A. V. 2009: Early Holocene volcanic ash fallout in the Yammoûneh lacustrine basin (Lebanon): tephrochronological implications for the Near East. *Journal of Volcanology and Geothermal Research 186*, 416–425.

Druitt, T. H., Edwards, L., Mellors, R. M., Pyle, D. M., Sparks, R. S. J., Lanphere, M., Davies, M. & Barreirio, B. 1999: Santorini Volcano. *Geological Society Memoir 19*, 165 pp.

Enzel, Y., Bookman, R., Sharon, D., Gvirtzman, H., Dayan, U., Ziv, B. & Stein, M. 2003: Late Holocene climates of the Near East deduced from Dead Sea level variations and modern regional winter rainfall. *Quaternary Research 60*, 263–273.

Fabbro, G. N., Druitt, T. H. & Scaillet, S. 2013: Evolution of the crustal magma plumbing system during the build-up to the 22-ka caldera-forming eruption of Santorini (Greece). *Bulletin of Volcanology 75*, https://doi.org/10.1007/s00445-013-0767-5.

Federman, A. N. & Carey, S. N. 1980: Electron microprobe correlation of tephra layers from Eastern Mediterranean abyssal sediments and the Island of Santorini. *Quaternary Research 13*, 160–171.

Giaccio, B., Hajdas, I., Isaia, R., Deino, A. & Nomade, S. 2017: High-precision ^{14}C and $^{40}Ar/^{39}Ar$ dating of the Campanian Ignimbrite (Y-5) reconciles the time-scales of climatic-cultural processes at 40 ka. *Scientific Reports 7*, 45940, https://doi.org/10.1038/srep45940.

Goldstein, S. L., Kiro, Y., Torfstein, A., Kitagawa, H., Tierney, J. & Stein, M. 2020: Revised chronology of the ICDP Dead Sea deep drill core relates drier-wetter-drier climate cycles to insolation over the past 220 kyr. *Quaternary Science Reviews 244*, 106460, https://doi.org/10.1016/j.quascirev.2020.106460.

Haase-Schramm, A., Goldstein, S. L. & Stein, M. 2004: U–Th dating of Lake Lisan (late Pleistocene Dead Sea) aragonite and implications for glacial east Mediterranean climate change. *Geochimica et Cosmochimica Acta 68*, 985–1005.

Hamann, Y., Wulf, S., Ersoy, O., Ehrmann, W., Aydar, E. & Schmiedl, G. 2010: First evidence of a distal early Holocene ash layer in Eastern Mediterranean deep-sea sediments derived from the Anatolian volcanic province. *Quaternary Research 73*, 497–506.

Heim, C., Nowaczyk, N. R., Negendank, J. F. W., Leroy, S. A. G. & Ben-Avraham, Z. 1997: Near East desertification: evidence from the Dead Sea. *Naturwissenschaften 84*, 398–401.

Hunt, J. B. & Hill, P. G. 1996: An inter-laboratory comparison of the electron probe microanalysis of glass geochemistry. *Quaternary International 34*, 229–241.

Jochum, K. P. and 52 others. 2006: MPI-DING reference glasses for in situ microanalysis: new reference values for element concentrations and isotope ratios. *Geochemistry, Geophysics, Geosystems 7*, Q02008, https://doi.org/10.1029/2005GC001060.

Kagan, E., Stein, M. & Marco, S. 2018: Integrated paleoseismic chronology of the last glacial Lake Lisan: from lake margin seismites to deep-lake mass transport deposits. *Journal of Geophysical Research: Solid Earth 123*, 2806–2824.

Keller, J., Ryan, W. B. F., Ninkovich, D. & Altherr, R. 1978: Explosive volcanic activity in the Mediterranean over the past 200,000 yr as recorded in deep-sea sediments. *Geological Society of America Bulletin 89*, 591–604.

Kitagawa, H., Stein, M., Goldstein, S. L., Nakamura, T. & Lazar, B. 2017: Radiocarbon chronology of the DSDDP core at the deepest floor of the Dead Sea. *Radiocarbon 59*, 383–394.

Kuehn, S. C., Froese, D. G. & Shane, P. A. R. 2011: The INTAV intercomparison of electron-beam microanalysis of glass by tephrochronology laboratories: results and recommendations. *Quaternary International 246*, 19–47.

Kuzucuoglu, C., Pastre, J. F., Black, S., Ercan, T., Fontugne, M., Guillou, H., Hatté, C., Karabiyikoglu, M., Orth, P. & Türkecan, A. 1998: Identification and dating of tephra layers from Quaternary sedimentary sequences of Inner Anatolia, Turkey. *Journal of Volcanology and Geothermal Research 85*, 153–172.

Kwiecien, O., Arz, H. W., Lamy, F., Wulf, S., Bahr, A., Röhl, U. & Haug, G. H. 2008: Estimated reservoir ages of the Black Sea since the last glacial. *Radiocarbon 50*, 99–118.

Landmann, G., Reimer, A., Lemcke, G. & Kempe, S. 1996: Dating Late Glacial abrupt climate changes in the 14,570 yr long continuous varve record of Lake Van, Turkey. *Palaeogeography, Palaeoclimatology, Palaeoecology 122*, 107–118.

Lane, C. S., Cullen, V. L., White, D., Bramham-Law, C. W. F. & Smith, V. C. 2014: Cryptotephra as a dating and correlation tool in archaeology. *Journal of Archaeological Science 42*, 42–50.

Lane, C. S., Lowe, D. J., Blockley, S. P. E., Suzuki, T. & Smith, V. C. 2017: Advancing tephrochronology as a global dating tool: applications in volcanology, archaeology, and palaeoclimatic research. *Quaternary Geochronology 40*, 1–7.

Limburg, E. M. & Varekamp, J. C. 1991: Young pumice deposits on Nisyros, Greece. *Bulletin of Volcanology 54*, 68–77.

Lowe, D. J. 2011: Tephrochronology and its application: a review. *Quaternary Geochronology 6*, 107–153.

Lowe, J. J., Ramsey, C. B., Housley, R. A., Lane, C. S. & Tomlinson, E. L. 2015: The RESET project: constructing a European tephra lattice for refined synchronisation of environmental and archaeological events during the last c. 100 ka. *Quaternary Science Reviews 118*, 1–17.

Machlus, M., Enzel, Y., Goldstein, S. L., Marco, S. & Stein, M. 2000: Reconstructing low levels of Lake Lisan by correlating fan-delta and lacustrine deposits. *Quaternary International 73–74*, 137–144.

Margari, V., Pyle, D. M., Bryant, C. & Gibbard, P. L. 2007: Mediterranean tephra stratigraphy revisited: results from a long terrestrial sequence on Lesvos Island, Greece. *Journal of Volcanology and Geothermal Research 163*, 34–54.

Matthews, I. P., Trincardi, F., Lowe, J. J., Bourne, A. J., MacLeod, A., Abbott, P. M., Andersen, N., Asioli, A., Blockley, S. P. E., Lane, C. S., Oh, Y. A., Satow, C. S., Staff, R. A. & Wulf, S. 2015: Developing a robust tephrochronological framework for Late Quaternary marine records in the Southern Adriatic Sea: new data from core station SA03-11. *Quaternary Science Reviews 118*, 84–104.

Migowski, C., Stein, M., Prasad, S., Negendank, J. F. W. & Agnon, A. 2006: Holocene climate variability and cultural evolution in the Near East from the Dead Sea sedimentary record. *Quaternary Research 66*, 421–431.

Narcisi, B. & Vezzoli, L. 1999: Quaternary stratigraphy of distal tephra layers in the Mediterranean—an overview. *Global and Planetary Change 21*, 31–50.

Neugebauer, I., Brauer, A., Schwab, M. J., Dulski, P., Frank, U., Hadzhiivanova, E., Kitagawa, H., Litt, T., Schiebel, V., Taha, N., Waldmann, N. D. & DSDDP Scientific Party 2015: Evidences for centennial dry periods at ~3300 and ~2800 cal. yr BP from micro-facies analyses of the Dead Sea sediments. *The Holocene 25*, 1358–1371.

Neugebauer, I., Brauer, A., Schwab, M. J., Waldmann, N. D., Enzel, Y., Kitagawa, H., Torfstein, A., Frank, U., Dulski, P., Agnon, A., Ariztegui, D., Ben-Avraham, Z., Goldstein, S. L., Stein, M. & DSDDP Scientific Party 2014: Lithology of the long sediment record recovered by the ICDP Dead Sea Deep Drilling Project (DSDDP). *Quaternary Science Reviews 102*, 149–165.

Neugebauer, I., Wulf, S., Schwab, M. J., Serb, J., Plessen, B., Appelt, O. & Brauer, A. 2017: Implications of S1 tephra findings in Dead Sea and Tayma palaeolake sediments for marine reservoir age estimation and palaeoclimate synchronisation. *Quaternary Science Reviews 170*, 269–275.

Paterne, M., Guichard, F. & Labeyrie, J. 1988: Explosive activity of the South Italian volcanoes during the past 80,000 years as determined by marine tephrochronology. *Journal of Volcanology and Geothermal Research 34*, 153–172.

Platevoet, B., Scaillet, S., Guillou, H., Blamart, D., Nomade, S., Massault, M., Poisson, A., Elitok, Ö., Özgür, N., Yağmurlu, F. & Yılmaz, K. 2008: Pleistocene eruptive chronology of the Gölcük volcano, Isparta Angle, Turkey. *Quaternaire 19*, 147–156.

Poli, S., Chiesa, S., Gillot, P.-Y., Gregnanin, A. & Guichard, F. 1987: Chemistry versus time in the volcanic complex of Ischia (Gulf of Naples, Italy): evidence of successive magmatic cycles. *Contributions to Mineralogy and Petrology 95*, 322–335.

Prasad, S., Negendank, J. F. W. & Stein, M. 2009: Varve counting reveals high resolution radiocarbon reservoir age variations in palaeolake Lisan. *Journal of Quaternary Science 24*, 690–696.

Prasad, S., Vos, H., Negendank, J. F. W., Waldmann, N., Goldstein, S. L. & Stein, M. 2004: Evidence from Lake Lisan of solar influence on decadal- to centennial-scale climate variability during marine oxygen isotope stage 2. *Geology 32*, 581–584.

Rossignol-Strick, M. 1995: Sea–land correlation of pollen records in the Eastern Mediterranean for the glacial–interglacial transition: biostratigraphy versus radiometric time-scale. *Quaternary Science Reviews 14*, 893–915.

Satow, C., Tomlinson, E. L., Grant, K. M., Albert, P. G., Smith, V. C., Manning, C. J., Ottolini, L., Wulf, S., Rohling, E. J., Lowe, J. J., Blockley, S. P. E. & Menzies, M. A. 2015: A new contribution to the Late Quaternary tephrostratigraphy of the Mediterranean: Aegean Sea core LC21. *Quaternary Science Reviews 117*, 96–112.

Schmincke, H.-U. & Sumita, M. 2014: Impact of volcanism on the evolution of Lake Van (eastern Anatolia) III: periodic (Nemrut) vs. episodic (Süphan) explosive eruptions and climate forcing

reflected in a tephra gap between ca. 14 ka and ca. 30 ka. *Journal of Volcanology and Geothermal Research 285*, 195–213.
Schmitt, A. K., Danišík, M., Aydar, E., Şen, E., Ulusoy, İ. & Lovera, O. M. 2014: Identifying the volcanic eruption depicted in a Neolithic painting at Çatalhöyük, Central Anatolia, Turkey. *PLoS ONE 9*, e84711, https://doi.org/10.1371/journal.pone.0084711.
Schmitt, A. K., Danišík, M., Evans, N. J., Siebel, W., Kiemele, E., Aydin, F. & Harvey, J. C. 2011: Acigöl rhyolite field, Central Anatolia (part 1): high-resolution dating of eruption episodes and zircon growth rates. *Contributions to Mineralogy and Petrology 162*, 1215–1231.
Siani, G., Sulpizio, R., Paterne, M. & Sbrana, A. 2004: Tephrostratigraphy study for the last 18,000 ^{14}C years in a deep-sea sediment sequence for the South Adriatic. *Quaternary Science Reviews 23*, 2485–2500.
Siebel, W., Schmitt, A. K., Kiemele, E., Danišík, M. & Aydin, F. 2011: Acigöl rhyolite field, central Anatolia (part II): geochemical and isotopic (Sr–Nd–Pb, δ^{18}O) constraints on volcanism involving two high-silica rhyolite suites. *Contributions to Mineralogy and Petrology 162*, 1233–1247.
St. Seymour, K., Christanis, K., Bouzinos, A., Papazisimou, S., Papatheodorou, G., Moran, E. & Dénès, G. 2004: Tephrostratigraphy and tephrochronology in the Philippi peat basin, Macedonia, Northern Hellas (Greece). *Quaternary International 121*, 53–65.
Stein, M. 2001: The sedimentary and geochemical record of Neogene-Quaternary water bodies in the Dead Sea Basin – inferences for the regional paleoclimatic history. *Journal of Paleolimnology 26*, 271–282.
Stein, M. & Goldstein, S. L. 2006: U–Th and radiocarbon chronologies of late Quaternary lacustrine records of the Dead Sea basin: methods and applications. *Geological Society of America Special Papers 401*, 141–154.
Stein, M., Ben-Avraham, Z. & Goldstein, S. L. 2011: Dead Sea deep cores: a window into past climate and seismicity. *Eos, Transactions American Geophysical Union 92*, 453–454.
Stein, M., Torfstein, A., Gavrieli, I. & Yechieli, Y. 2010: Abrupt aridities and salt deposition in the post-glacial Dead Sea and their North Atlantic connection. *Quaternary Science Reviews 29*, 567–575.
Stockmarr, J. A. 1971: Tablets with spores used in absolute pollen analysis. *Pollen et Spores 13*, 615–621.
Sumita, M. & Schmincke, H.-U. 2013a: Impact of volcanism on the evolution of Lake Van I: evolution of explosive volcanism of Nemrut Volcano (eastern Anatolia) during the past >400,000 years. *Bulletin of Volcanology 75*, https://doi.org/10.1007/s00445-013-0714-5.
Sumita, M. & Schmincke, H.-U. 2013b: Impact of volcanism on the evolution of Lake Van II: temporal evolution of explosive volcanism of Nemrut Volcano (eastern Anatolia) during the past ca. 0.4 Ma. *Journal of Volcanology and Geothermal Research 253*, 15–34.
Tomlinson, E. L., Arienzo, I., Civetta, L., Wulf, S., Smith, V. C., Hardiman, M., Lane, C. S., Carandente, A., Orsi, G., Rosi, M., Müller, W. & Menzies, M. A. 2012a: Geochemistry of the Phlegraean Fields (Italy) proximal sources for major Mediterranean tephras: implications for the dispersal of Plinian and co-ignimbritic components of explosive eruptions. *Geochimica et Cosmochimica Acta 93*, 102–128.
Tomlinson, E. L., Kinvig, H. S., Smith, V. C., Blundy, J. D., Gottsmann, J., Müller, W. & Menzies, M. A. 2012b: The Upper and Lower Nisyros Pumices: revisions to the Mediterranean tephrostratigraphic record based on micron-beam glass geochemistry. *Journal of Volcanology and Geothermal Research 243–244*, 69–80.
Tomlinson, E. L., Smith, V. C., Albert, P. G., Aydar, E., Civetta, L., Cioni, R., Çubukçu, E., Gertisser, R., Isaia, R., Menzies, M. A., Orsi, G., Rosi, M. & Zanchetta, G. 2015: The major and trace element glass compositions of the productive Mediterranean volcanic sources: tools for correlating distal tephra layers in and around Europe. *Quaternary Science Reviews 118*, 48–66.
Torfstein, A. & Enzel, Y. 2017: Dead Sea lake level changes and Levant palaeoclimate. *In* Bar-Yosef, O. & Enzel, Y. (eds.): *Quaternary of the Levant: Environments, Climate Change, and Humans*, 115–126. Cambridge University Press, Cambridge.
Torfstein, A., Goldstein, S. L., Kagan, E. J. & Stein, M. 2013a: Integrated multi-site U–Th chronology of the last glacial Lake Lisan. *Geochimica et Cosmochimica Acta 104*, 210–231.
Torfstein, A., Goldstein, S. L., Kushnir, Y., Enzel, Y., Haug, G. & Stein, M. 2015: Dead Sea drawdown and monsoonal impacts in the Levant during the last interglacial. *Earth and Planetary Science Letters 412*, 235–244.
Torfstein, A., Goldstein, S. L., Stein, M. & Enzel, Y. 2013b: Impacts of abrupt climate changes in the Levant from Last Glacial Dead Sea levels. *Quaternary Science Reviews 69*, 1–7.
Torfstein, A., Haase-Schramm, A., Waldmann, N., Kolodny, Y. & Stein, M. 2009: U-series and oxygen isotope chronology of the mid-Pleistocene Lake Amora (Dead Sea basin). *Geochimica et Cosmochimica Acta 73*, 2603–2630.
Vinci, A. 1985: Distribution and chemical composition of tephra layers from Eastern Mediterranean abyssal sediments. *Marine Geology 64*, 143–155.
Waldmann, N., Stein, M., Ariztegui, D. & Starinsky, A. 2009: Stratigraphy, depositional environments and level reconstruction of the last interglacial Lake Samra in the Dead Sea basin. *Quaternary Research 72*, 1–15.
Wick, L., Lemcke, G. & Sturm, M. 2003: Evidence of Lateglacial and Holocene climatic change and human impact in eastern Anatolia: high-resolution pollen, charcoal, isotopic and geochemical records from the laminated sediments of Lake Van, Turkey. *The Holocene 13*, 665–675.
Wulf, S., Hardiman, M. J., Staff, R. A., Koutsodendris, A., Appelt, O., Blockley, S. P. E., Lowe, J. J., Manning, C. J., Ottolini, L., Schmitt, A. K., Smith, V. C., Tomlinson, E. L., Vakhrameeva, P., Knipping, M., Kotthoff, U., Milner, A. M., Müller, U. C., Christanis, K., Kalaitzidis, S., Tzedakis, P. C., Schmiedl, G. & Pross, J. 2018: The marine isotope stage 1–5 cryptotephra record of Tenaghi Philippon, Greece: towards a detailed tephrostratigraphic framework for the Eastern Mediterranean region. *Quaternary Science Reviews 186*, 236–262.
Wulf, S., Keller, J., Paterne, M., Mingram, J., Lauterbach, S., Opitz, S., Sottili, G., Giaccio, B., Albert, P. G., Satow, C., Tomlinson, E. L., Viccaro, M. & Brauer, A. 2012: The 100–133 ka record of Italian explosive volcanism and revised tephrochronology of Lago Grande di Monticchio. *Quaternary Science Reviews 58*, 104–123.
Wulf, S., Keller, J., Satow, C., Gertisser, R., Kraml, M., Grant, K. M., Appelt, O., Vakhrameeva, P., Koutsodendris, A., Hardiman, M., Schulz, H. & Pross, J. 2020: Advancing Santorini's tephrostratigraphy: new glass geochemical data and improved marine-terrestrial tephra correlations for the past ~360 kyrs. *Earth-Science Reviews 200*, 102964, https://doi.org/10.1016/j.earscirev.2019.102964.
Wulf, S., Kraml, M., Brauer, A., Keller, J. & Negendank, J. F. W. 2004: Tephrochronology of the 100 ka lacustrine sediment record of Lago Grande di Monticchio (southern Italy). *Quaternary International 122*, 7–30.
Wulf, S., Kraml, M. & Keller, J. 2008: Towards a detailed distal tephrostratigraphy in the Central Mediterranean: the last 20,000 yrs record of Lago Grande di Monticchio. *Journal of Volcanology and Geothermal Research 177*, 118–132.
Wulf, S., Kraml, M., Kuhn, T., Schwarz, M., Inthorn, M., Keller, J., Kuscu, I. & Halbach, P. 2002: Marine tephra from the Cape Riva eruption (22 ka) of Santorini in the Sea of Marmara. *Marine Geology 183*, 131–141.
Zanchetta, G., Sulpizio, R., Roberts, N., Cioni, R., Eastwood, W. J., Siani, G., Caron, B., Paterne, M. & Santacroce, R. 2011: Tephrostratigraphy, chronology and climatic events of the Mediterranean basin during the Holocene: an overview. *The Holocene 21*, 33–52.

Supporting Information

Additional Supporting Information may be found in the online version of this article at http://www.boreas.dk.

Table S1. Excel file of EPMA glass geochemical data (raw and normalized, volatile-free) of Lateglacial cryptotephra from the ICDP Dead Sea core and glass standards measurements (raw data).